Multidimensional NMR and Data Processing

ISTVÁN PELCZER*,† and SÁNDOR SZALMA‡

NMR and Data Processing Laboratory, Chemistry Department, CST Bldg., Syracuse University, Syracuse, New York 13244, and Inst. für Organische Chemie, J. W. Goethe—Universität Frankfurt, Niederurseler Hang, D-6000 Frankfurt am Main, Germany

Received April 30, 1991 (Revised Manuscript Received August 1, 1991)

Contents

István Pelczer is the Operations Manager of the NMR & Data Processing Laboratory at Syracuse University (Syracuse, NY) where he came at the invitation of G. C. Levy in 1988. He holds Master's and Ph.D. degrees in Chemistry from "József Attilla" University, Szeged, Hungary. After completing his Master's in 1978 he was associated with EGIS Pharmaceuticals and Drug Research Institute (both in Budapest, Hungary) as a research NMR spectroscopist. During this time he collaborated with Pál Sohár. He has also worked as a visiting scientist in the laboratories of J. K. M. Sanders (University of Cambridge, Cambridge, U.K., in 1984) and Ad Bax (NIH, Bethesda, MD, in 1989). His main research interest is in multidimensional NMR applications, including experimental and data processing developments.

Sándor Szalma is a Research Assistant at J. W. Goethe University, Frankfurt am Main, Germany, working with C. Griesinger since 1990. He completed his graduate training in Chemistry at "József Attila" University, Szeged, Hungary in 1984. Then he joined G. Bernáth's laboratory at "Szent-Györgyi A." Medical University, Szeged, Hungary, where he received the Ph.D. degree in Chemistry. He worked as a postdoctoral fellow at Syracuse University (Syracuse, NY) with G. C. Levy during 1989–1990. His research interest is in multidimensional NMR spectroscopy with particular emphasis on the computational aspects of NMR data processing and high-performance algorithms.

I. Introduction

High-resolution multidimensional (*n*D, i.e. more than two dimensional) nuclear magnetic resonance spectroscopy was a great challenge of the late 1980s, and probably is the most exciting field of applications in the 1990s.

Theoretical extension of dimensionality to more than two was mentioned at the beginning of multidimensional era (i.e. data acquisitions as a function of more than two independent time parameters).[1] However, at this time many scientists did not put much confidence even in 2D NMR, primarily because of concerns about data processing difficulties. Problems with data size, transposition, processing speed, evaluation, as well as advantageous separation of acquisition and data pro-

† Syracuse University.
‡ J. W. Goethe—Universität Frankfurt.

0009-2665/91/0791-1507$09.50/0

cessing had already been discussed.[2] Development of reliable hardware,[2] theoretical background and sophisticated experimental techniques[3,4] in two-dimensional NMR, as well as revolutionary improvement of computation[5-7] was necessary to realize nD NMR.

Three-dimensional NMR spectroscopy is widely applied already, involving double and triple resonance experiments.[8-14] Extension to the fourth dimension,[15] and lately full 4D experiments have been carried out.[16-19] Further variants have also been proposed.[20,21] Five-dimensional experiments are said to be on the way, and maybe 6D is not far away either.

This review discusses data processing in multidimensional pulsed Fourier transform NMR spectroscopy,[8] including some recent applications of reconstruction methods, which are becoming increasingly popular. In the following we will be focusing on problems occurring primarily in multiple-, i.e. in more than two dimensional, NMR spectroscopy. However, many of these problems, suggested solutions, and ways of data handling are general and have some commonalty with two-dimensional NMR spectroscopy, especially when the enormous size of data is the origin of difficulties.

We have tried to touch all major points of multidimensional NMR spectroscopy which are closely connected to data processing steps. Preacquisition and experimental considerations affecting data handling and data processing possibilities are briefly surveyed. Acquisition schemes, data storage and format, and processing strategies are also subjects of this work. Data processing procedures, already familiar from two-dimensional applications, as well as those specific for multidimensional applications are discussed. Visualization and evaluation of spectra are mentioned. Details on instrumentation and computer hardware are discussed only marginally since these are subjects of a very fast development.

Stochastic NMR spectroscopy represents a special, promising territory in multidimensional NMR.[22] For example, the information present in a 3D correlation spectrum is available from 3D sections cut through 5D or even 7D stochastic spectra.[8] Since data acquisition and data processing methodology is much different from that of pulsed Fourier transform nD NMR spectroscopy, the reader is referred to existing literature.[22]

In order to exploit the full 3D multiplex advantage, it is desirable to record 3D spectra that cover the entire spectral range in all the three dimensions,[8] and this is so for higher dimensions, as well. Of course, experiments frequently involve selective, or semiselective excitations ("soft" experiments) both to simplify the spectrum and reduce size, experiment time and data processing difficulties. One of the first high-resolution 3D experiments was a double "soft"-COSY spectrum.[23] Its final output size was (after zero filling) 256 × 256 × 4096 (real) points, and the processing took 7 h on an Aspect 1000 computer using home-written software (Figure 1).

Selective excitation experiments, extendable into multidimensions,[24] will be discussed elsewhere in this issue.[25] Application of selective pulses instead of time incrementation provides information of reduced dimensionality, as is common in image spectroscopy. Also, there are experiments, involving extra dimensions hidden, as relay type parts,[26] isotope filtering[11] or as extra decoupling.[15] Such practical approaches result in less severe problems in size and complexity of the data.[27] On the other hand, experimental problems from appropriate selective excitation and the limited amount of information extracted are some of the disadvantages.

The other possibility, to acquire data with time-domain incrementation in each dimension, is always a matter of compromise. Acquisition time, instrumentation, stability of sample, size of output data, etc. are the factors limiting multidimensional experiments. Experimental tricks, data processing manipulations, and other optimization approaches are of extreme importance. Of course, the information content of multidimensional spectra is usually huge, providing access to investigation of structures larger and more complex than ever before.[13,14,28]

Increasing data size is a straightforward consequence of increasing the number of dimensions. It poses direct storage problems,[10,29] as well as difficulties in data transfer and processing. Certain kinds of experiments may even require linear combinations of separately stored subsets of nD data, as has already been used for isotope-filtered spectra in 2D.[30] An elegant approach uses a linear combination of appropriately acquired TOCSY derivatives in order to increase signal to noise.[31,32]

Massive disk storage capacity is inevitable for nD experiments, mainly if oversampling[33] is carried out in the detected dimension to improve the dynamic range of the experiment. On the other hand, efforts have been made to decrease the number of acquired points to a minimum through extensive folding[34,35] or appropriate linear prediction of data.[36] An interesting theoretical consequence of increasing resolution by increasing the number of dimensions, is that an experiment of N dimensions may require fewer independent FIDs to acquire than one of dimensionality $(N - 1)$.[20]

Off-line processing has come to play a more important role than ever before, as a straightforward consequence of high computational demands. Sophisticated versions of independent data processing software are available on the market, usually developed to have close connections to data evaluation and structure calculation programs. Highly parallel computation[37] is becoming more and more important.[38,39] We will not go into details of available software, graphics, and other computer hardware, instead, the reader is referred to recent literature.[5,6,7,39,40]

If published data are cited we prefer to follow the classification as it has originally appeared in the literature. For example, we shall use TOCSY[41] or HOHAHA[42] following the original publication.

II. Preacquisition Considerations

Appropriate data processing begins with proper data acquisition. Careful planning and optimization for multidimensional NMR spectroscopy of larger molecules is extremely important.[43,44] Maximization of sensitivity and minimization of measuring time,[34,45] as well as the possibilities and limitations of further data manipulations are critical.

A. Experiment Time and Artifacts

Multidimensional acquisitions often compromise on artifact suppression in order to minimize the necessary

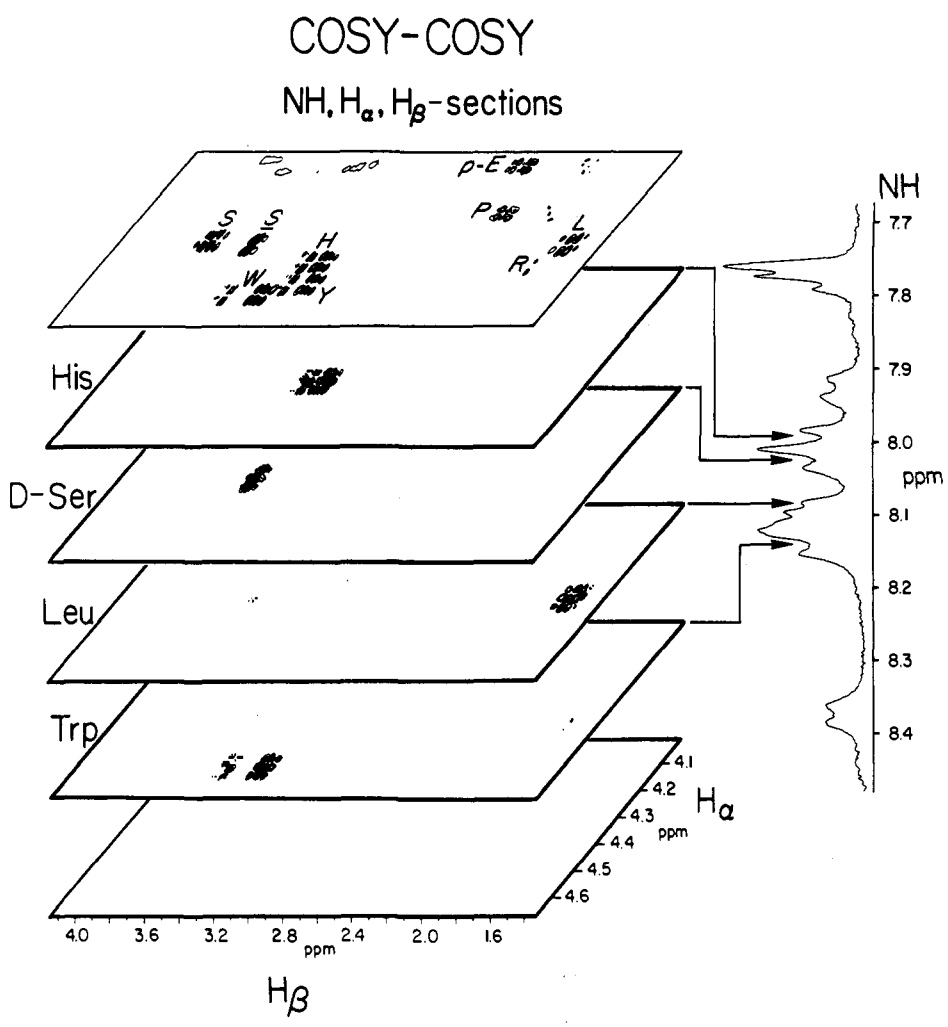

Figure 1. Three-dimensional COSY-COSY spectrum of 70 mM buserilin in DMSO-d_6. Four 2D cross sections of the 3D spectrum parallel to the $\omega_2(C_\alpha H)$ and $\omega_3(C_\beta H)$ axes are shown at NH frequencies of His, D-Ser, Leu, and Trp, respectively. Acquisition size was 96 × 96 × 2048 (real) points. The spectral width is 500 × 500 × 3000 Hz. Contours are drawn for both positive and negative intensities (reprinted from ref 23; copyright 1987 American Chemical Society).

number of scans per increment and reduce the size of the output data. As a straightforward consequence of this situation, optimizing experimental conditions, highly reliable instrumentation, as well as artifact suppression through data processing become even more critical than in 2D NMR.

In most applications of multidimensional NMR the minimum number of scans required is limited by necessary phase cycling rather than by sensitivity. Although this area does not bear directly on data processing, minimization of necessary phase cycling steps should be remembered.[46] Experimental effort can be further reduced in cases when certain experimental procedures can be replaced with data processing steps. For example, signals of uniform phase difference, such as dispersive diagonal peaks in phase-sensitive COSY spectra can be removed through data manipulation.[47]

B. Sampling

Sampling in time is linear in common cases where sampling rates define frequency ranges to be detected according to the well-known Nyquist relation. However, there are other interesting possibilities. Oversampling[33,48] can be used for multidimensional acquisitions[49] to reduce dynamic range problems and to filter folded noise in indirectly detected dimensions even though it enlarges the data size considerably.

Nonlinear sampling is another very interesting possibility. Exponential sampling has already been demonstrated to be useful in two-dimensional NMR.[50,51] The drawback of this approach at present is that it requires MEM reconstruction, but this is less a problem as computational power increases. In addition to shortening experimental time, nonlinear sampling offers data compression. Such compressed data would be easier to transfer through long distance networks.

C. Quadrature Detection Methods, Acquisition Schemes

Absorption-mode presentation of multidimensional spectra, if applicable, has general advantages.[52] Some guidelines to the type of FT and spectrum display for a nD experiment have been discussed.[8] If pure absorption profiles can be obtained in all the dimensions, then a full phase sensitive calculation and display is the right choice in order to exploit maximum capacity of the results. When phase distortions or inherently mixed peak shape occur in one or more dimensions, absolute value presentation is necessary after discarding imaginaries in dimensions exhibiting pure absorption profiles. Such mixed mode presentations have also been used in 2D processing to improve resolution of the final spectrum.[53,54]

Phase-sensitive detection is commonly linked to sign discrimination (quadrature detection). Simultaneous versus sequential acquisition[2] in the acquired dimension, and choices in the implementation of quadrature detection in indirectly detected dimensions are not the same. The two different methods have been comparatively analyzed.[52] Redfield[55] and TPPI[56-58] or hypercomplex[59,60] methods, as well as a special combination of the two (States-TPPI)[46,61] can be applied. Possible acquisition schemes reported so far differ in terms of simultaneous or sequential acquisition of the orthogonal magnetization components and addition/subtraction of results as a part of the acquisition process or of data processing.[46,62] The type of FT (real versus complex) to be applied, as well as the position of axial peaks in the resulting spectrum, are different. If axial peaks are located out of the spectral range of interest, their suppression is not necessary, saving experimental time.

Artifacts in correlation spectra,[62] as well as folding (aliasing),[63] are closely determined by the type of acquisition scheme and Fourier transform method being applied. Although simultaneous and sequential type acquisition schemes are very closely related,[52,60] the TPPI approach has some disadvantages in practice. For "real" or TPPI type acquisitions the long tails of the dispersive part of each component with negative frequency may lead to severe base-line distortions in the positive frequency region.[64] This makes correct phasing impossible in some cases and results in increased ridges and other artifacts. On the other hand, folding (aliasing) properties of complex data are advantageous in terms that shifting of the virtual carrier position is possible during data processing.[65] Appropriate postacquisition shifting of carrier frequency has been carried out, for example, for the ^{13}C (F2) dimension in the 3D NOESY-HMQC spectrum of calmodulin to bring all the aliphatic resonances within the observed spectral window.[66] As a result, spectral windows can be limited to the minimum size; only direct overlap should be avoided due to cancellation.

At present, the best strategy for acquisition data in indirectly detected dimensions seems to be the States-TPPI method,[46] which has been used for various multidimensional acquisitions[43,67] with success. TPPI mode quadrature detection in all dimensions is, however, still widely used in multidimensional NMR.[68,69] One of the most likely reasons is that only the latest models of commercial NMR spectrometers are flexible enough to freely choose the acquisition scheme.

Block structure (relative locations of reals and imaginaries) of the output nD FID is determined by choice of appropriate phase programs to select desired coherence transfer pathways. There are two systematic approaches using either "preparatory phases" or "detection phases";[8] however, several other combinations are possible. The nD processing software should be flexible enough to handle any of these. The user should be given options for combining real and imaginary blocks, as well as capability for any mixed variants of TPPI and/or complex data structure for powerful nD processing.

D. First Delays in Indirectly Detected Dimensions

In the acquisition dimension a delay is introduced between the last pulse and the first acquired point in time to avoid pulse breakthrough and other hardware problems.[2] Introduction of an echo-type read pulse sandwich[70] and detection of sine modulation signals using sequential acquisition scheme[71] were proposed to avoid base-line problems arising from imperfect measuring conditions and thus reducing the necessity in difficult base-line correcting procedures. In the latter case first point correction is not necessary either. By careful experiment setup base-line problems can be reduced even to the level when no correction by software is necessary. For example, extra base-line correction was avoided for a 3D HMQC-NOESY-HMQC spectrum by adjusting the receiver phase to give sine modulation, as well as through careful gating of the receiver and proper tuning of the first delay.[71]

First points in indirectly detected dimensions do not suffer such deviations, but still are affected by both incorrect scaling by discrete Fourier transform and delayed sampling. Both introduce base-line distortions, which cannot be reduced sufficiently by scaling.[72] Linear prediction of the missing point after setting the first effective delay exactly at one dwell time[73] is possible. Then halving of the first point's intensity to compensate overestimation by the FT procedure is still necessary. This procedure needs careful adjustment of experimental parameters, as well as increased computation with FT and IFT steps.[73]

Beginning data acquisition at exactly half dwell time appears to be the most powerful approach so far.[61,74] This method has several advantages: no scaling of the first point(s) is necessary, the base line is largely distortionless, and aliasing is easy to follow. When complex data are acquired, acquisition delayed by half dwell time results in aliased peaks exactly antiphased in comparison with those ones falling within the detected range[74] (Figure 2).

This well-defined phase relationship is very important when time-domain data are to be extended by linear prediction[36] (see later). When only a few points are acquired and maximum acquisition time is on the order of the dwell time the half dwell time approach provides some valuable extra resolution.

E. Buffered Acquisition

Disk I/O time becomes an important factor as nD experiments are usually run acquiring only a few scans per file with relatively short recycling delays and dummy scans are frequently avoided. Overhead time may in fact double the actual experimental time needed if dummy scans are also involved.[75] For example, 47 out of 177 h were used just for I/O procedures for a 3D NOESY-HMQC experiment with acquisition size of 100 × 37 × 1024 (all complex) data points.[76] In a 119-h 3D HOHAHA-NOE experiment on a Bruker AM-500 spectrometer 58 h were spent on disk transfers and reloading of the pulse programmer.[77] Data size was 246 × 256 × 512 real points. Therefore it was necessary to modify the acquisition computer to permit buffered acquisition.[46] This allows in-memory acquisition of many actual FIDs without writing them on the disk, saving considerable time for data transfer. Dummy scans should be avoided, too, if possible. Uniform starting conditions for each cycle can be provided by using spin-lock or homospoil-like pulses in between

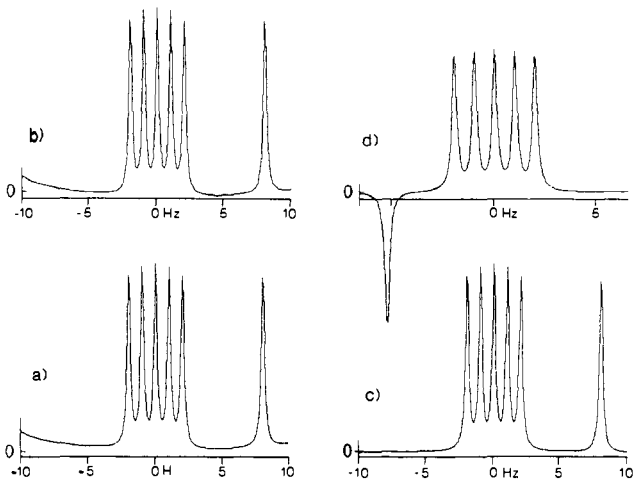

Figure 2. Simulated spectra obtained by Fourier transformation of data with an initial sampling delay of $^1/_4$ dwell time. For a multiplication of the first data point by 0.75 was used, and for b the scaling factor was 0.6. For both a and b the linear phase correction was 90° across the spectrum. Part c shows a spectrum obtained for a sampling delay equal to one-half dwell time, with no scaling of the first data point. Part d shows a spectrum obtained if the spectral window is narrowed by 33%. The resonance at the right side of the spectrum is aliased and appears inverted at the left-hand side. For both c and d the linear phase correction is 180° (reprinted from ref 74; copyright 1991 Academic Press.).

acquisitions.[46] Another approach is to accomplish all evolution time incrementations before changing subsequent phase cycling steps.[78,79]

III. Postacquisition Manipulations

Data processing in the more conventional meaning occurs, of course, after acquisition is completed. In the following, we'll survey the major steps, and also some extensions and variants of currently available methods in order to get reasonable frequency domain information. Until now, multidimensional spectra were processed mostly with home-written software[69,77,80-84] or in combination with existing commercial software.[45,49,67,71,85-89]

A. Processing Strategies

Output format and structure of the acquired data is a function of the acquisition mode; acquisition scheme and relative phase shifts to obtain quadrature detection[8] (see also above). These characteristics largely determine the processing strategies to apply. Data size and access to the particular dimensions, phase properties, noise distribution, visualization strategy, etc., must always be considered during setting up processing protocols.

It seems to be the most straightforward way to process the data in successive steps, as is usual for 2D. However, even for 2D spectra it might be worth beginning with the indirectly detected dimension, as, for example, when linear prediction (replacement) of the first point(s) is applied in t_2.[73]

Since most multidimensional correlations involving one or more heteronuclear axes are analyzed by using homonuclear 2D slices, filtered by heteronuclei (e.g. ^{15}N or ^{13}C) the algorithm which renames files instead of transposing them physically (see later) is especially advantageous.[61] Following this strategy, the heteronuclear dimension is processed first including (calculated) phase correction. Then homonuclear 2D slices can be handled with commercial processing software.[61] Selected slices can be zero filled in the usual way.

Although this strategy seems to be the most developed one for such spectra at this time, other approaches are also possible. Processing 3D NOESY-HMQC spectra has been reported,[76] for example, transforming the $\omega_1 - \omega_3$ (NOESY) planes first, and—after base-plane correction—finishing data processing with FT in t_2.

If homonuclear correlations are combined (e.g. COSY, HOHAHA, NOESY, etc.), processing cross sections perpendicular to the acquisition dimension[68,83,84] may have the following advantages. The spectral resolution and usually the digital resolution is the highest in this domain. Cross talk between the planes is, therefore, less severe than in any of the other dimensions. Also, noise distribution in these perpendicular planes is more uniform than that in other slices.[77,90] A possible convenient choice is to process and analyze only selected slices of interest after the acquisition dimension has been Fourier transformed. Selectivity for slice selection can be improved through appropriate zero filling, however, overall size increases.

Selective processing using SDFT[91] (see later) is another choice, with complete flexibility, which sets the limits of selectivity back to that determined only by the spectral resolution.

B. Data Access, Transposition

Data access could be the very limiting bottleneck of processing in many instances. To access any point or slice of a multidimensional dataset equally quickly on a one-dimensional medium (like the hard disk of computer) it is practical to organize the data in a format that enables the system to accomplish this efficiently. By using so called sequential data storage, the FIDs or 1D spectra stored one after the other, incrementing the other dimension is inefficient. By using this, one would face the problem of corner turning,[92] i.e. transposing the dataset to have quick access in other dimensions. Such processing slows down the overall procedure, requires extra storage space, and becomes more complicated with an increasing number of dimensions. A powerful method has been proposed to avoid one transposition step in 3D processing.[61] This method applies renaming of files using bit reversal and the "butterfly algorithm" rather than physically transposing them (Figure 3).

The improvement in speed and convenience is remarkable; to reach the stage having the appropriate t_1 – F2 – t_3 dataset of initial size (128 × 2) × (32 × 2) × (256 × 2) points took about 1.5 h on a Sun-4-110 workstation, without visual inspection and in local mode.[61] Further, regular 2D processing can be accomplished by using commercial software. Appropriate F2 slices can be selected for applying extensive zero filling without a penalty on overall size. It is not, however, a general solution, and for visualization in orthogonal planes it is impractical and inefficient.

In order to avoid transposition for multidimensional processing, a data structure based on submatrices can be used instead,[84] allowing fast access to data in all dimensions. This approach, the so-called "brick" method, has found its place successfully in commercial NMR software (UXNMR of Bruker, FELIX of Hare Research, and TRIDENT[174]) and even in molecular modelling

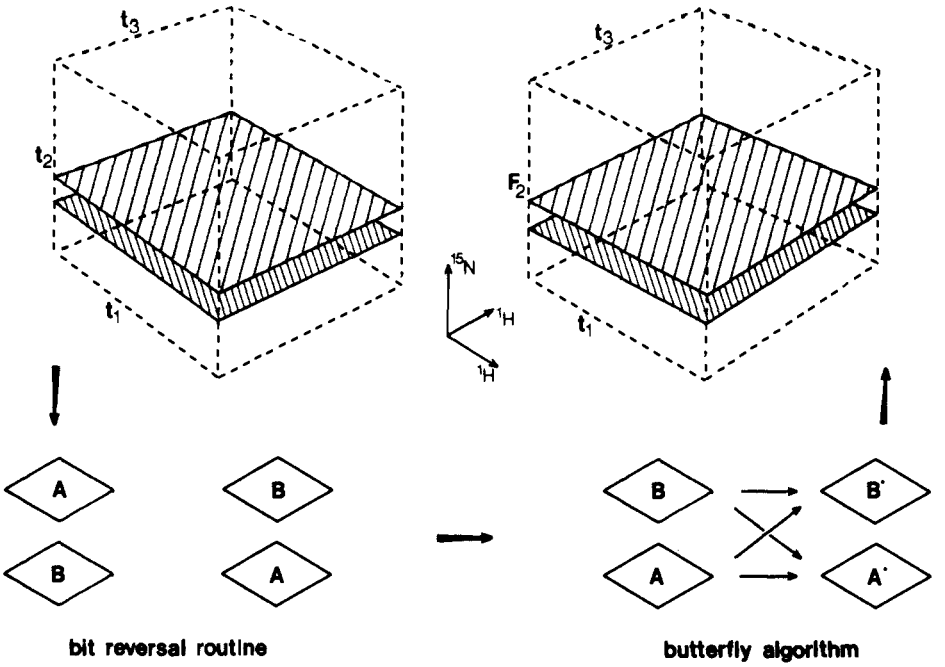

Figure 3. Schematic representation of the Fourier transform process in t_2. Each (t_1, t_3) plane is manipulated according to the prescription for each point in a 1D transform. The transform is divided into two sections. The first consists of a bit reversal routine whereby the planes are renamed appropriately. The planes are then recombined according to the "butterfly algorithm"[118] to generate a (t_1, F2, t_3) data set[61] (reprinted from ref 61; copyright 1989 Academic Press).

(QUANTA of Polygen). Nonsequential data storage (brick method) has extra advantages if parallel processing or distributed processing should be utilized. It is worth mentioning that selective processing (SDFT, see later)[91] is also an alternative to avoid limitations of sequential data storage and access.

C. Extension of Time-Domain Data by Linear Prediction

The number of acquired data points, especially in indirectly detected dimensions, is usually quite limited for multidimensional NMR spectroscopy. This is so not only because of data size limitations, but also as a consequence of experimental difficulties (sample and instrumental stability, etc.). Even fast acquisition methods[46] do not give a general solution to this problem. Usually the resulting spectrum lacks sufficient resolution, which can not be changed drastically by the usual interpolation (zero filling). Moreover, as truncation should be avoided, strong weighting (see later) suppresses valuable data points at the end of the FID, decreasing sensitivity.

Linear prediction (LP) methods, which are subjects of another chapter of this issue,[93] can be applied for reasonable extension of time domain data. Such extension can be carried out in a straightforward manner,[94] calculating real and imaginary components independently in the positive time regime. Safe limits for LP extension of time domain data are a function of the number of acquired data points, number of frequency domain components, as well as the relative noise level. Instabilities are clearly visible upon increasing number of predicted points (Figure 4).

As an application of this approach, direct extension of 192 acquired (TPPI) points to 484 points in each of the indirectly detected dimensions for a 3D TOCSY–TOCSY spectrum by linear prediction to get better line shape through optimized apodization has been reported.[95] For a recently published four-dimensional data set the following LP extensions have been reported:[17] 36 to 44 points in t_1, 128 to 160 points in t_2, and 32 to 40 points in t_3, all real points. This experiment is a good example of concerted use of conventional experimental, as well as data processing efforts for optimized results.

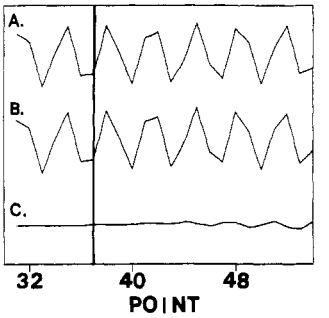

Figure 4. Comparison of real (A) and predicted (B) time-domain data. The first 36 data points were used to predict 18 additional points in B. The difference between the actual data and the predicted data is shown in C. The data are from a t_1 interferogram of a two-dimensional NOE experiment on the small peptide Pro(10)-AAP(7-23) (reprinted from ref 94; copyright 1990 Academic Press).

It is preferable to reduce the number of variables for linear prediction calculations from the original four (frequencies, amplitudes, phases, and damping factors) to two.[36] If complex data are acquired with first point at half dwell time, the phase of all signals can be predicted.[74] Also, damping of sinusoids for seriously truncated data, which is often the case for multidimensional experiments, is usually negligible. Slight corrections can be made applying line sharpening apodization functions, if necessary.[36] Appropriate calculations include reflection of increasing roots into the unit circle and mirror image projection procedure to the negative time regime, as well. Following this procedure, time-domain size can be extended by a factor of 4.[36] Using such processing acquisition of only eight (com-

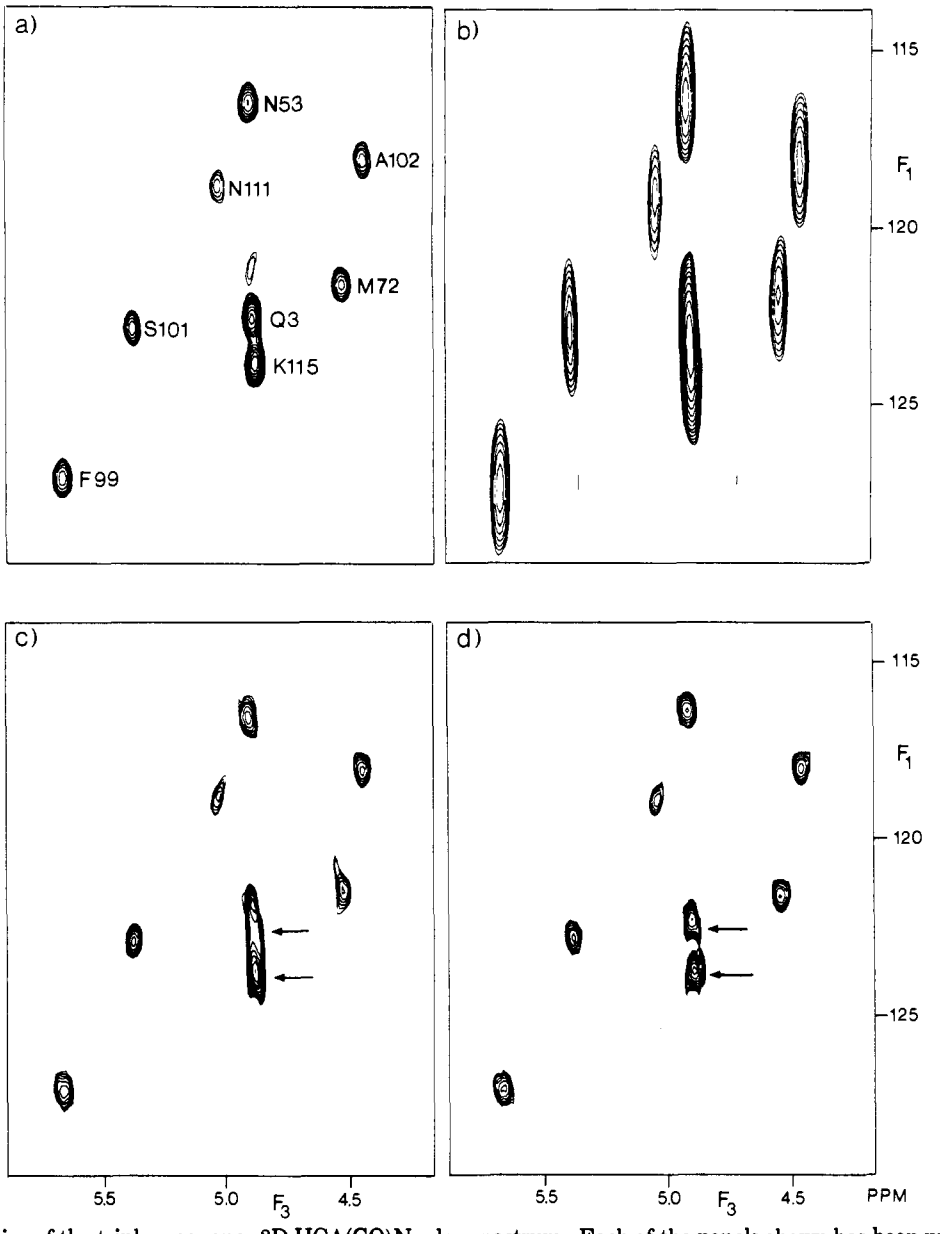

Figure 5. (F1, F3) slice of the triple-resonance 3D HCA(CO)N relay spectrum. Each of the panels shown has been processed identically in the F3 dimension: (a) Fourier transform obtained after 9-Hz exponential line narrowing followed by cosine^2-bell apodization of 32 complex t_1 time-domain data points and zero filling to 128; (b) same as a, but using only the first 8 t_1 time-domain data points; (c) spectrum obtained by 9-Hz exponential line narrowing, linear prediction of the first 8 data points out to 32 followed by cos^2-bell apodization, zero filling, and Fourier transformation; (d) processed like c, but using the negative plus positive time domain data points (16 complex data) for linear prediction of the additional 24 points. The arrows in c and d mark the true F1 coordinate of the Q3 and K115 resonances as observed in a (reprinted from ref 36; copyright 1990 Academic Press).

plex) points may result in practically equivalent resolution as if 32 complex data points were acquired (Figure 5).

Extension of 32 complex points to 64 by linear prediction in one of the ^{15}N dimensions for a ^{1}H–^{15}N HMQC/(^{1}H–^{1}H NOESY)^{15}N–^{1}H HMQC experiment has been reported.[96] The same strategy has been applied successfully to 4D heteronuclear correlations as well, reducing necessary experiment time remarkably.[18,19]

This is a general technique, however, limited by the number of resonances being present in the actual slice to be processed. For this reason, all the other dimensions are usually transformed before application of LP extension of time-domain data and successive inverse Fourier transform steps are applied if necessary[18,19] (Figure 6).

Doubly heteronuclear-filtered 4D (and even 5D, etc.) experiments are good candidates for this strategy, as the number of resonances in a single heteronuclear slice is usually low due to the extremely high selectivity.[18,19] Similar calculations for more crowded spectra need computational development.

D. First Point Correction

First points may be distorted by acquisition, but also the FT algorithm may overestimate their value (see also later). It is common to multiply these first points with an appropriate factor,[72] frequently optimized in a trial and error procedure for the acquisition dimension. Since indirectly detected dimensions usually do not suffer from experimental errors the theoretical factor 0.5[72] can be used in most cases, when effect of finite

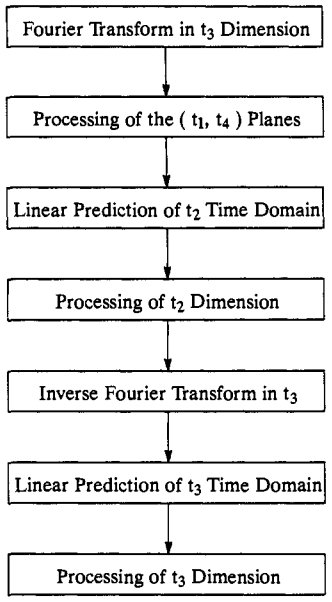

Figure 6. Flowchart of the steps used for processing a 4D spectrum involving linear prediction extension of time-domain data in two dimensions (reprinted from ref 19; copyright 1991 Academic Press).

pulse widths can be neglected. However, if half dwell time was used for the first point, no multiplication is necessary.[74]

E. Apodization

In multidimensional NMR the maximum acquisition time is seriously limited at least in the indirectly detected dimensions. As a consequence, time-domain signals are usually strongly truncated. The main purpose of apodization is therefore to decrease this effect to a reasonable level. At the same time, sensitivity, as well as resolution, should be retained as much as possible. For heteronuclear dimensions with a size of only few points, unusual apodization functions have been proven to be appropriate. For example, a doubly shifted sinusoid[16,61,67,88] retains both reasonable line shape and sensitivity. As an alternative, a shifted sinebell/exponential broadening combination[10] has been proposed (Figure 7).

For example, 45° shifted sinebell and 400-Hz exponential line broadening combined apodization has been used for the carbon dimension in a 3D ^{13}C–^{1}H–^{1}H HSMQC-NOESY spectrum (75) with 67 Hz/point final digital resolution. Other apodization functions serve the same purpose. For example, a Hamming window has been reported for a homonuclear 3D NOE-NOE spectrum.[83]

There is a special situation when a slight damping of the time-domain frequency components should be compensated to make appropriate linear prediction extension of the time domain data possible.[36] Then, an exponential line sharpening function should be applied prior to LP. Of course, when the extended time domain data are subject to further (in fact, conventional) processing, the apodization functions, mentioned above, will be used.

F. Phase Correction

One of the rationales for the large data sizes produced in multidimensional NMR is to be able to combine the

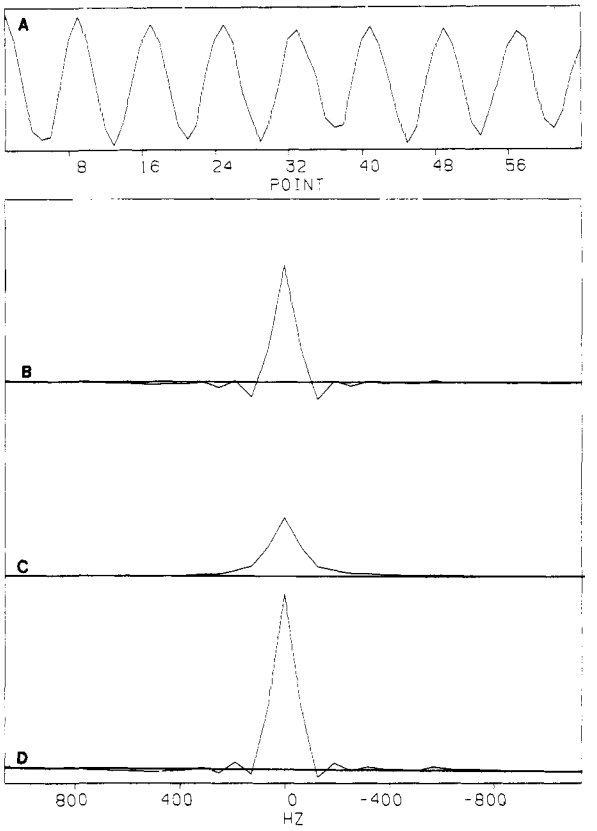

Figure 7. The top panel shows a typical interferogram as obtained for the ^{15}N dimension of a 3D experiment. The data shown in the top panel transformed with a sine bell 45 window function is shown in panel b, with a line broadening of 150 Hz (panel c), and with the addition of the two apodization functions (panel d) (reprinted from ref 10; copyright 1990 Cambridge University Press).

real and imaginary data achieving a "good" absorptive spectrum. This phase correction can be done through automated procedures, as was proposed for 2D spectra having diagonal elements.[97] It can be based on a 1D DISPA procedure[98–100] or its 2D version.[101] Of course, manual phase correction is always a possibility.[102]

If the phase properties of 2D spectra from which the 3D (*n*D) was composed are known, it is possible to predict the 3D peak shapes for different types (cross, back-transfer, cross-diagonal, diagonal).[8] Then, choosing orthogonal 1D vectors, phasing can be accomplished in successive steps.[9] A serious drawback of this approach is that in order to save time and memory space, the imaginaries are usually discarded before the next consecutive step. If phase correction has not been sufficient in an early step, it may be difficult to restart processing from the beginning.

Zolnai et al.[103] have proposed a very useful strategy to avoid this problem. They suggest to compute only the real part of the spectrum (in 2D 4-fold, in 3D 8-fold size reduction, etc.) and then reconstruct the imaginaries applying the Hilbert transform.[104] Phase corrections for each dimension are accomplished independently and successively. This procedure saves both processing time and storage space as the imaginary parts are present as necessary. The results are quite promising. It was possible to process and phase correct a medium-size 3D spectrum on an Intel 80386 based PC with array processor within 10–90 min.

Another practical alternative is to use selective reconstruction (SDFT)[91] of 1D slices for the purpose

finding appropriate phase correction parameters. By SDFT, phasing can be carried out in all dimensions, cycling through appropriate 1D slices. Thus necessary parameters can be determined before the total, or even partial, transformation of the dataset. Mistaken phase parameters can be detected and replaced in an early stage of processing, sparing much computation time.

It is worth mentioning here, that in certain cases, as for antiphase cross-peak structure and low resolution, a defined alteration in phase correction ("twist"[105,106]) results in some gain in sensitivity.[105]

G. Zero Filling, Digital Resolution

Zero filling once prevents loss of half of the information acquired.[63,107] Otherwise zero filling is usually considered as a merely cosmetic action to obtain visually better looking spectra. Theoretically spectral resolution is what inherently limits the available information, but in practical cases zero filling can make of that information more available.

Adding extra zeros to the end of the acquired (or maybe already extended by LP,[36,94] see above) FID works as a type of generalized curve/surface fitting on the whole spectrum, according to the characteristics of the FID and filtering being applied. Such a procedure is definitely the most convenient, although not necessarily the most exact, approach, as different peaks may have very different behavior.[108] Locally different parameters can be applied with selective processing[91] when one also is free to alter the digital resolution (see later).

None of these approaches increase the theoretical information content of the spectrum. However, for either further visual or automated data handling, some level of zero filling is advantageous in comparison with individual curve/surface fit analysis for each region with reasonable intensities. Systematic errors of integration of a discrete NMR spectrum can be reduced by appropriate zero filling, as was shown for 1D spectra.[109] Also, reconstruction methods such as MLM[110,111] may lead to better results if digital resolution is improved.[112]

H. Base-Line Distortion and Corrections

Base-line (base-plane) distortions originate from two major sources: erroneous scaling by the algorithm being applied for Fourier transformation[72,113] and experimental mismatches. The latter case incorporates several possible sources of error. If, for example, the required zero-order phase correction is not a multiple of 90° for time-domain data acquired in sequential mode, real Fourier transformation results in nonlinear base-line distortions.[64] This can be overcome by setting the relative phase of the receiver and the transmitter properly.[64] Problems of the first data point(s)[114] and delayed acquisition can be corrected either by pure experimental efforts, including echo-type read pulse sandwich[70,115,116] if applicable, or by concerted use of appropriate timing and linear prediction of missing points.[73] Linear prediction of the first point(s) can be accomplished when acquisition has begun at exactly the first dwell time point;[73] however, this timing is not too critical. The method can be used to correct distorted first point(s) in any FIDs followed by phase correction. As only few points are necessary to extrapolate, the fast Burg algorithm[117,118] can be used instead of the classical singular value decomposition method (LPSVD).[119] This extrapolation should be done after Fourier transformation is accomplished in the orthogonal dimension(s) to reduce the number of frequency domain components and avoid lengthy calculations.[73]

MEM reconstruction of the spectrum (see also later) or LPSVD reconstruction of the distorted first part of time domain data[113] might also be subjects of interest. Cosine fit of the base line is an alternative approach.[120] This method effectively removes the base-line roll caused, for example, by delayed acquisition. Such delays usually occur in selective excitation experiments[8] and heteronuclear correlations. It is effective even with noisy data, without affecting the first points of the FID. This can be important for later integration, since the vast majority of information about integrals are in first points, Moreover, this method works very well with Gaussian line shapes, making this line shape the superior choice for base-line correction and integration for multidimensional NMR.[80]

More conventionally, a (higher order) polynomial base-line fit also can be used, either in between consecutive Fourier transformation steps, or after all are complete. The former approach is usually inevitable when noncompensated selective pulses have been used in the sequence.[8] However, such manipulations should be applied with care, as imperfect base-line compensations can introduce further nonuniform modulation of the time-domain signals. Various base-line corrections, applied on 3D spectra, have been reported in the literature.[75-77,121]

Recently a two-dimensional Cardinal spline method was also shown to effectively remove F2 ridges and other artifacts from distorted 2D NMR spectra.[122] Extension of this approach to multidimensions is feasible, although it might be very time consuming.

It should be reemphasized that, if first point detection at half dwell time was applied,[74] base-line correction in indirectly detected dimensions is not necessary in most cases.

I. Suppression of Residual (Water) Signal

Probably the most frequently occurring base-line distortions originate from residual solvent (water) signal. It may be desirable to remove such residual signal for other reasons as well.

In many cases the H_2O signal, surviving presaturation or other suppression maneuvers, gives a dispersive signal in the detected dimension. It can be removed in the frequency, or in the time domain. In the frequency domain, techniques involve conventional base-line fitting, and in its more sophisticated version subtracting also the dispersive component.[123] Absorption phased residual signal is easy to remove, and after Hilbert reconstruction of the imaginary part a highly distortion-free spectrum can be regained.[124] This strategy has also been published in a more generalized version to remove two-dimensional signals of uniform phase difference, compared to the (cross-)peaks of interest.[47]

Residual signal of any phase can be removed effectively in the time domain. The idea is based on "base-line correction" of the FID[125] suppressing certain, usually low frequency contributions. Versions either in differential[126,127] or the more sophisticated integral form[128] have been developed. The Karhunen–Loëve

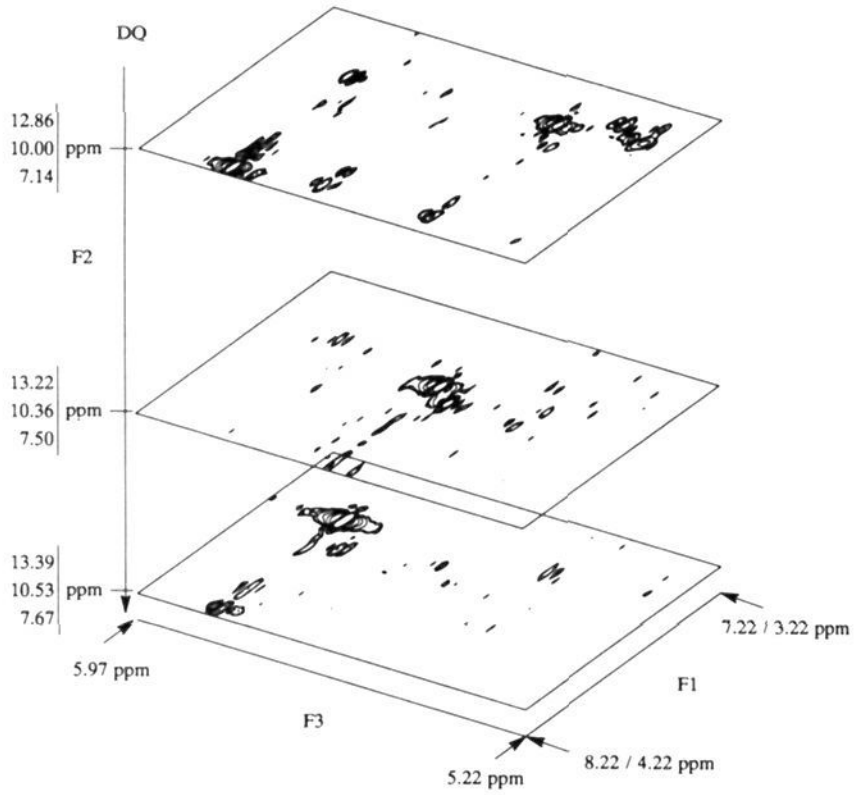

Figure 8. Three-dimensional NOESY/DQ-COSY correlation for a 24-mer RNA hairpin structure[173] processed by SDFT. Selected NOESY (F1–F3) slices are shown. Data were acquired in hyper-hypercomplex mode in four blocks. Acquisition size was 1024 × 32 × 64 ($t_3 - t_2 - t_1$, all complex) points. Result of a local increase in digital resolution ("zoom") is demonstrated. Only a preselected area (F1 – F3; base – 1′ NOESY correlations) was reconstructed. Output size was only 240 × 31 × 62 (real) points, which corresponds to an increase of digital resolution by factors of 2, 1, and 3.9, respectively. Similar increase by conventional processing would result in output size of 2048 × 32 × 256 points.[133]

digital signal filtering in the time domain[129] is especially useful for 3D NMR. This technique relies on creating an autocorrelation matrix and finding the eigenvalues. Substantial data compression is afforded by removing the smallest eigenvalues (which belong to noise).[130] If the method is applied to select and remove the largest eigenvalues (which in turn belong to the solvent signal), the result is a virtually solvent-free 3D spectrum.[131]

J. Selective Discrete Fourier Transformation

Selective Discrete Fourier Transformation (SDFT)[91] is a powerful alternative to the widely used FFT algorithm in many cases. Advantageous features are most pronounced in multidimensional spectroscopy. In direct comparison, SDFT is slower than FFT on the same data set if the size is larger that 32 points. However, if a limited range is the only subject of interest, which is often the case for multi-dimensional spectra, the overall time can be remarkably less. Also, if suitable hardware (DSP chips, parallel computers) and machine-optimized matrix multiplications are used, performance can be increased impressively.

The method is actually an up-to-date revival of the traditional spectrum analyzer[63] using submatrix multiplications.[132] Selectivity may include either reconstruction of a limited frequency range, lower dimensional subvolumes, slices, surfaces in nD, or reconstructions with arbitrarily fewer or more frequency domain points than defined by the acquisition. In regard to the latter point, local digital resolution can be increased without the penalty of a huge output size[133] (Figure 8).

This can be very useful, for example, when fine digitization is required in a multidimensional spectrum to measure coupling constants.[11,29] Instead of subvolume(s), special planes can also be presented without reconstruction of any other part of the frequency domain spectrum (Figure 9).

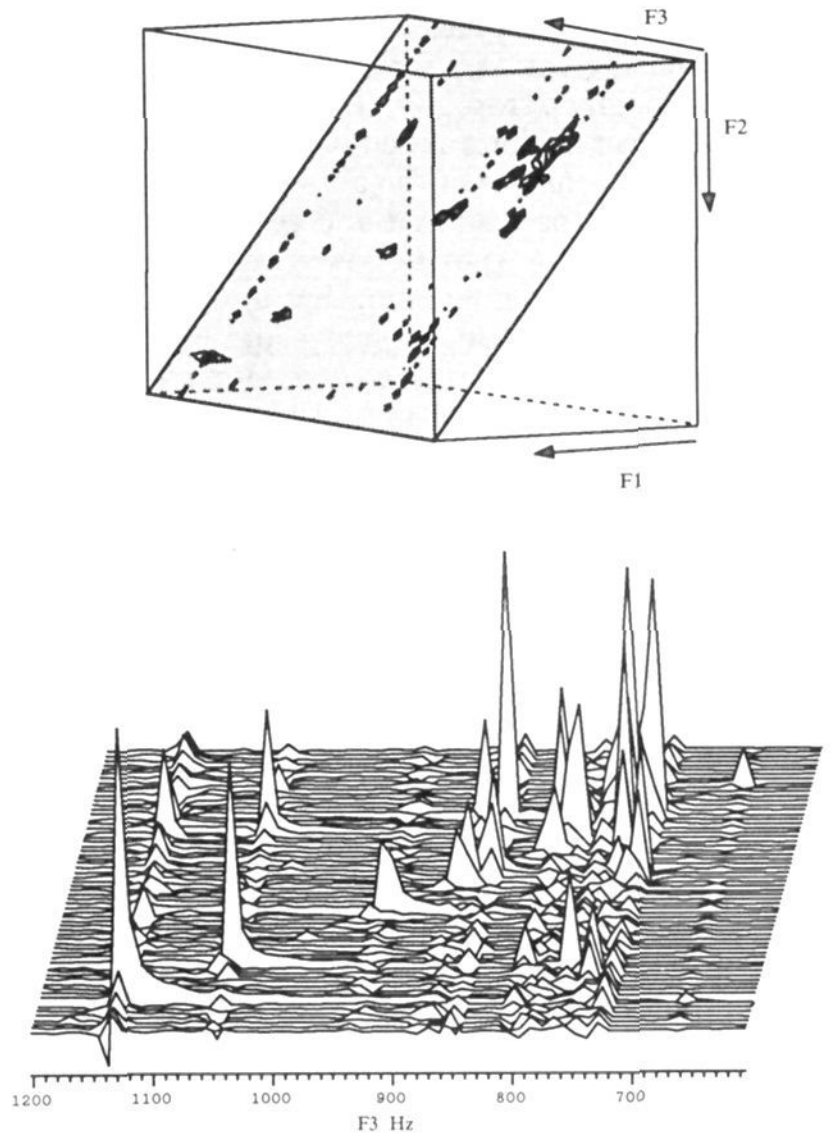

Figure 9. The F1 = F2 cross-diagonal plane (top) and the corresponding stacked plot (bottom) from the homonuclear ROESY-HOHAHA spectrum of benzanthracene.[151] The reconstruction was carried out selectively; only the shown part was calculated. The time-domain data size was 32 × 64 × 256 (all complex; t_1, t_2, t_3) points. The resulting spectrum contains 64 × 128 real points, and it took 77 s of CPU time on a Stellar GS-1000 graphics supercomputer to reconstruct[91] (reprinted from ref 91; copyright 1991 Academic Press).

Locations of output frequency domain points are defined by look-up tables using SDFT processing.[91] Consequently, digital resolution can be lower than that defined by the time domain size (a kind of oversampling). This leads to fast and convenient preprocessing options, as phase correction and optimization of other processing parameters concerted in nD, as well as the possibility to have a quick look at interesting region(s) even before processing is started on the whole spectrum. Parameters can be *locally different* or, on the other hand, *different* parameters for the *same* region can be tested in one step.

The higher the number of dimensions or the larger the overall size of data, the more advantageous is the application of the SDFT processing. Combination of this approach with various other techniques, as deconvolution methods, could be very promising.

K. Processing Alternatives to FT

There are many errors connected with conventional FT processing. Usual problems for multidimensional (and therefore nonideally detected) spectra are low resolution, noise, phase and base-line errors partially due to first point problems, leaking (wiggles), etc. Reconstruction of multidimensional NMR spectra

based on non-Fourier transformation methods is, consequently, a subject of increasing interest, despite their usually huge computational demands and other practical problems.

Several approaches have been introduced in the NMR literature which have been recently thoroughly reviewed.[93,113,134-138] Maximum entropy (MEM)[113,134-136] and maximum likelihood (MLM)[110] reconstruction, as well as linear prediction (LP) methods[93,113,134] are being used more widely to improve data processing. However, the huge computational demands mentioned before are still serious limitations for direct use on larger data sets, as nD spectra. There are some possible ways to ease this problem. Combination of the above methods with selective processing methods, as SDFT[91] can reduce the overall size of the required data, while still retaining reasonable digital resolution. Another possible approach is application of huge computational power and massive parallelism,[37] most likely in developed computer centers through networking.[39] Further developments in the algorithms applied may also result in faster and less complicated computation.

IV. Enhancement of Frequency-Domain Data

A. Removal of Artifacts

Multidimensional spectra usually suffer nonsuppressed artifacts, as a result of keeping the number of scans per file as small as possible. Several experimental, as well as straightforward data processing efforts can be made to decrease these effects (see above).

Postprocessing data treatment may involve application of principal component analysis (PCA), as was shown for 2D spectra.[139] It was found that in removing the largest principal components it is possible to suppress the main sources of variance in data, i.e. base-line offset, base-line roll, t_1 noise, quadrature images, etc. The computation time requirements are reasonable, falling into the same range as Fourier transformation.

Recently a method, using linear prediction, has been proposed to remove oscillatory artifacts caused by truncation of free induction decay.[140] This approach might be possible to apply to more than two-dimensional cases.

B. Resolution Enhancement

Multidimensional spectra usually show much less overlap than those of lower dimensionality.[16-19] However, application of constrained deconvolution methods, as maximum entropy (MEM[113]) and maximum likelihood (MLM[110,111]) methods, is a promising data processing alternative in resolving crowded spectra (Figure 10).

Currently no existing software works in more than two dimensions, and there are also practical limitations is size. The largest MLM applications, according to our best knowledge, work on a $2K \times 2K$ real-point 2D correlation spectrum at the time,[141] although this limitation will be eased by introduction of massive parallelism[37] in computation of NMR spectra.[39]

Recently a linear prediction based method, so-called LP-ZOOM has been introduced, for detailed analysis of a selected frequency region of an NMR spectrum.[142] Here the spectral refinement starts from the z domain[142] which, in certain circumstances, is the same as the frequency domain. This method has proven to be useful; however, it was also shown that LP-ZOOM cannot be applied without restrictions, and it's performance is dependent on the nature of the spectrum to be analyzed.[143]

C. Symmetry

Symmetry relationships is more than two dimensions are not obvious, are more complicated than in most 2D applications, and closely depend on the nature of magnetization transfer processes.[8,9,144] Even in the case when symmetry should be present given the magnetization transfer steps, experimental circumstances (very different acquisition times, resolution, etc. in different dimensions) often destroy this inherent symmetry. As a consequence, symmetrization routines, frequently used in 2D NMR, are not appropriate for 3D (nD) NMR. However, an inversion symmetry exists for $^{13}C/^{13}C$-edited homonuclear proton NOESY 4D correlations[17,18] for example, which could be used to improve spectral quality.

D. Data Compression

Data reduction is aimed at reducing the overall size of the data and the associated computational and mass storage demands. The reduction can be accomplished at different stages of the procedure. Preacquisition considerations and proper organization of the experiment (see above) may lead to reduced output data size. Straightforward steps can be also taken during the processing. Imaginaries can be thrown away after proper phasing in the dimension in question.[61] A reduced "strip" of the data set, already processed in the previous domain(s), can be selected and transformed to produce a smaller dataset.[9] This "strip" selection has been available in the Bruker software for a long time and can be applied also in nD NMR processing.[17] The approach can be generalized for reasonable data compression and straightforward automation if the TRAWIATA algorithm is followed.[145] If rephasing is necessary, Hilbert transformation is a convenient tool to reconstruct the imaginary part again.[103,104] Involvement of Hilbert transformation into multidimensional processing saves not only storage space, but also computer time[103] according to the actual I/O performance.

Artifact and solvent suppression in already processed spectra[146] combined with data compression is possible for purposes of future handling.[139,147] This is especially straightforward if data are already reduced to the dynamic range level of the cross peaks.[47] Such compressed data can be used in well-organized data analysis software, as in PIXI,[148] even on small personal computers. The final reduction level is to save the spectrum as only a "peak table" information set, from which the whole spectrum can be reconstructed if necessary.[149] However, the latter solution should be used only with care as real spectra are always far from an ideal and well-characterized peak set.

V. Visualization of Multidimensional Spectra

A. Storage Problems

In visualizing a 3D (nD) spectrum there are few possible solutions for data storage. One is to store the

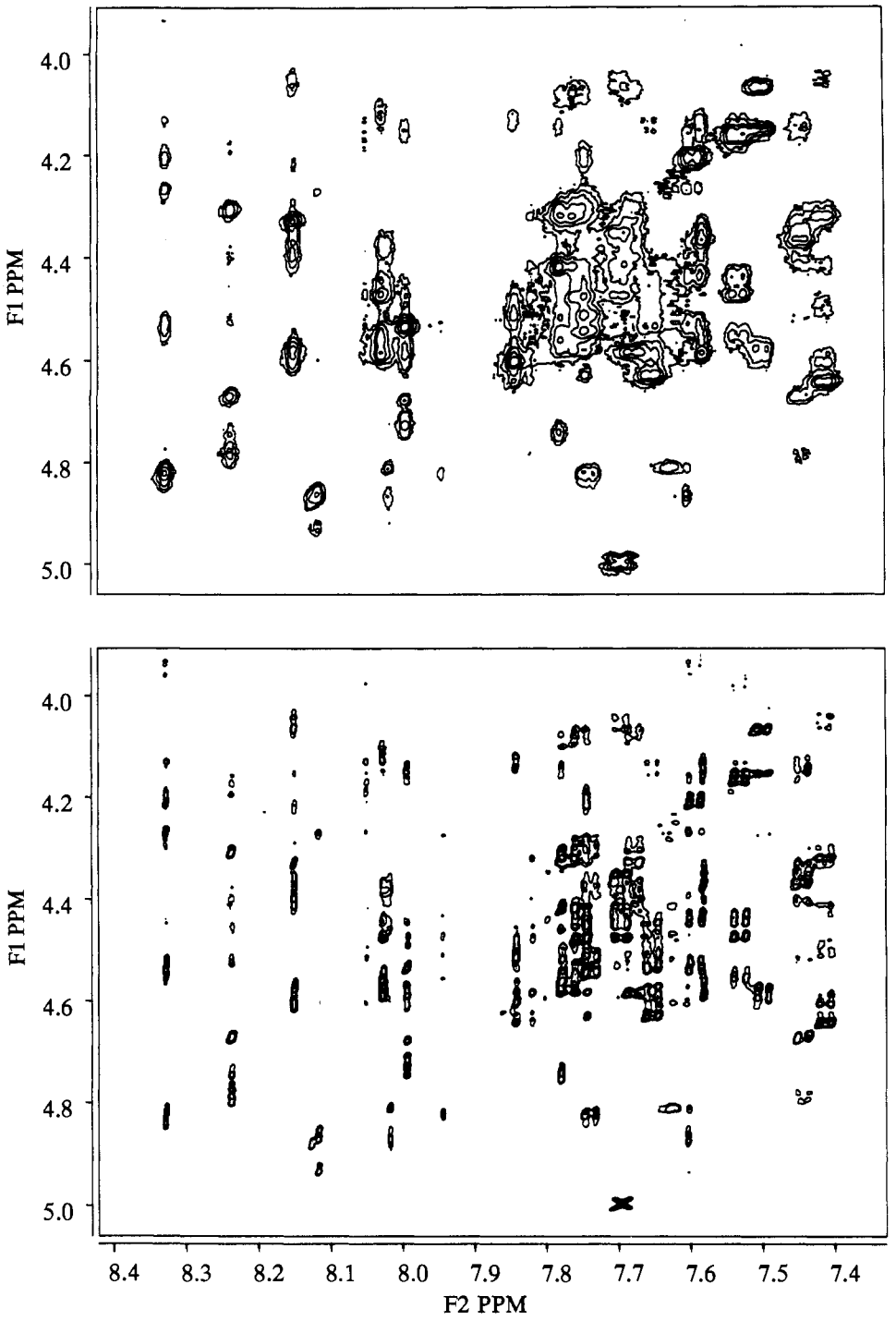

Figure 10. Results of MLM-after-symmetrization processing (SML) on a base-to-2′ subregion of the 2D NOESY spectrum of a 24-mer RNA hairpin structure:[173] (a) conventional processing and (b) MLM reconstruction. The original 4K × 512 (hypercomplex) spectrum was zero filled 4K × 4K, diagonally symmetrized by replacing each related point by the minimum of the absolute values retaining the original sign. The presented 1K × 1K subregion was extracted and reconstructed by MLM with 100 iterations and -6 Hz line sharpening. Overlapping is greatly decreased, while relative volumes of peaks are conserved.[112] (The spectra are courtesy of P. N. Borer and G.-w. Jeong.)

data continuously in main memory of the computer. This can be a costly solution taking into account the prices for large and fast random access memory (RAM). Such storage may need RAM being at least 30% or even two times larger than the total data size in order to avoid disk swapping (a standard process on widely used computers and operating systems). Room is needed also for other purposes (the program itself needs space, operating system, etc.), especially in a multiuser environment. All this may end up with the requirement of 32–128 Mbyte RAM size for a moderate range of 16–64 Mbyte data size. The other practical solution is to have only partial data stored in RAM: typically 2–12 Mbyte (for which the RAM size should be 8–16 Mbyte). The remaining part resides on the disk. In this case the program should refresh the dataset in RAM through explicit disk requests. This still can pose a serious load on the system, for even mainstream disk drives and computers/operating systems. However it is a cheaper, and not much slower solution, and there is no upper size

limit other than background memory. Also, for 3D data it may be very practical to reformat a stack of planes into small subcubes,[10] to have fast access to any cross sections.

Recently published 4D spectra are huge (e.g. 1.2 Gbyte[17]) and even after processing are still beyond the size which can be easily handled by the mainstream workstations (e.g. 1.6 Gbyte[17] and 134 Mbytes,[18] respectively). Therefore some kind of selective processing and partial presentation is inevitable, even with rapidly increasing computational power.[39]

B. Space Views

Presentation of a whole 3D spectrum as a space view, for example a homonuclear nonselective 3D spectrum[84] is more valuable aesthetically than from the point of view of real data evaluation (Figure 11).

However, such space veiw presentation may still be appropriate for general information about spectral features. Evans and Sutherland graphics stations have been widely used for display and presentation,[8,9,81,150] although any other graphics software can be used for the same purpose as well. Stereoviews of contour plots in 3D, possibly in perspective mode[151] may be presented. Of course, no higher dimensional spectra can be visualized in a similar way.

C. Plane Hopping

Although it seems to be a simplification, a mutual plot of appropriate 2D slices, selected from the nD correlation solid seems to be the most convenient and most practical solution. Connectivities can be followed from plane to plane in various directions—"plane hopping".[87] Such presentations easily follow appropriate data processing, when only selected planes are transformed in the last step (see above). As the virtual position of the carrier can be changed at will for indirectly detected dimensions acquired in hypercomplex mode,[61,74] selected 2D slices of a multidimensional correlation solid are easy to match for convenient visual evaluation. Such 2D slices from 3D spectra can be plotted with simple contouring software which creates xy plots or Postcript files as outputs for laser printers.[88]

"Plane hopping" is probably the most widely used presentation/evaluation method at the time. For example, 2D planes for inspection of a nonselective 3D NOE-HOHAHA for an oligosaccharide have been shown.[68] An elegant example of how to use selected 2D planes to evaluate connectivities on a 3D spectrum has been shown for a 3D HMQC-COSY spectrum of kanamycin A.[152] Planes selected from several 3D spectra can be combined, of course. Such concerted evaluation of five independently acquired different 3D spectra has been presented for calmodulin[12] (Figure 12).

VI. Approaches for Evaluation

A. Manual Connectivity Search

Manual evaluation of multidimensional spectra is extremely time consuming and difficult, with plane hopping the most straightforward approach. Although increasing the number of dimensions may introduce some confusion, reducing peak overlap is advantageous.

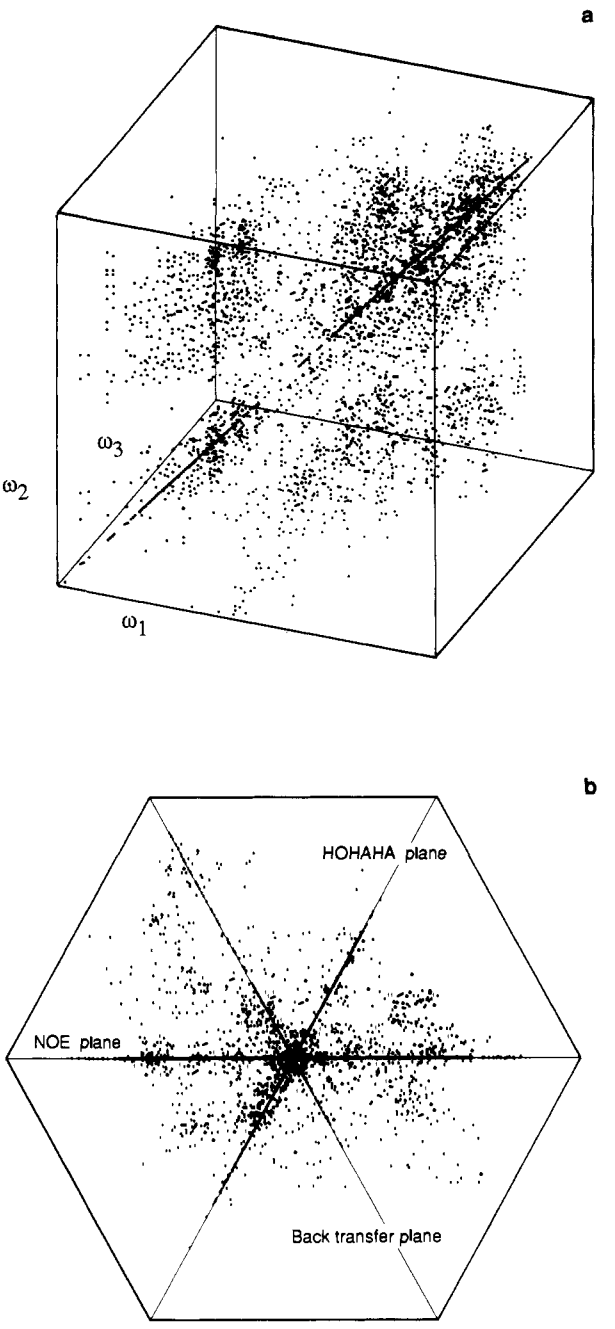

Figure 11. Three-dimensional NOE-HOHAHA spectrum of 8.7 mM pike parvalbumin (pI = 5.0). Parts a and b show only a limited number of local maxima for the spectrum. The plane containing the t_1 and t_2 noise of the strong H_2O resonance was eliminated. Panel a shows the view of the 3D NOE-HOHAHA spectrum, and panel b shows the view along the diagonal axis ($\omega_3 = \omega_2 = \omega_1$) of the cube (reprinted from ref 84; copyright 1988 Academic Press).

B. Approaches toward Automated Evaluation

Automated analysis of (two-dimensional) correlation spectra is usually approached by two main strategies. One of them analyzes the detailed fine structure of cross-peaks, while the other focuses on connectivities, determined from relatively low-resolution spectra. Combination of 2D spectra into multidimensional solids for improved data analysis and data banking has already been proposed.[153] A very similar strategy, which uses 2D spectra corresponding to projections from a heteronuclear 3D correlation, has been applied to au-

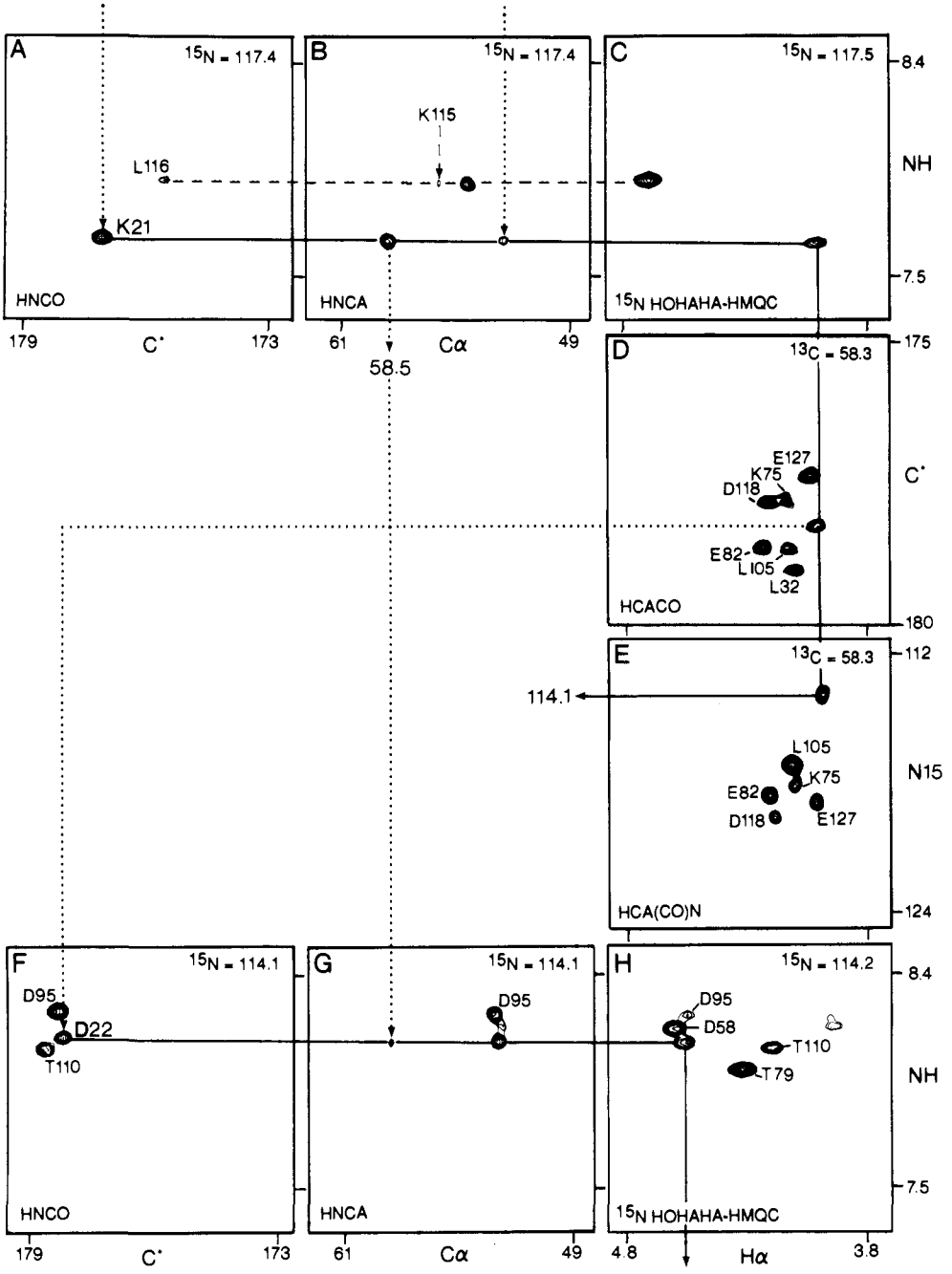

Figure 12. Selected regions of slices from five separate 3D NMR experiments for calmodulin.[12] These regions illustrate the J correlation between Lys-21 and Asp-22. Solid and dotted lines trace the connectivity patterns for these two residues. Slices A–C are taken at the Lys-21 ^{15}N chemical shift. Slices D and E are taken at the Lys-21 C^{α} shift, observed in B. Slices F–H are taken at the ^{15}N frequency of Asp-22, as measured in E[12] (reprinted from ref 12).

tomated three-dimensional sorting of 2D cross-peaks of protein spectra.[154] Such strategies can be transposed to higher dimensional cases, as well.

Sequential multidimensional homonuclear and heteronuclear magnetization transfer experiments, especially those with in-phase multiplet structures, are excellent candidates for automated spectral evaluation. The large number of 3D cross-peaks in such correlations (ca. 10^5) makes some kind of automation desirable anyway. On the other hand, reduced overlap due to increased dispersion by adding dimensions results in easier recognition of individual cross-peaks. Fine structure of peaks in a 3D spectrum can be informative.[144,155] However, low resolution is inherent for many applications, especially for larger molecules where lines are broad. Consequently, connectivities are more often used to get structural information. Automated peak picking from a multidimensional spectrum in combination with path analysis methods[153,156] is a promising strategy. Application of high capacity neural network systems would be also desirable.

Attempts to develop strategy and concrete software for spectral evaluation at a high level of automation have been made.[10,157] Also a program has been developed for the evaluation of 3D spectra and has been applied to the sequential assignment of BPTI utilizing a 3D TOCSY-NOESY correlation.[158] A semiautomatic assignment strategy has been developed and used with success for sequential assignment of calmodulin.[12] The process involves combining information from several 3D spectra and strongly resolution enhanced 2D heteronuclear correlations (Figure 13).

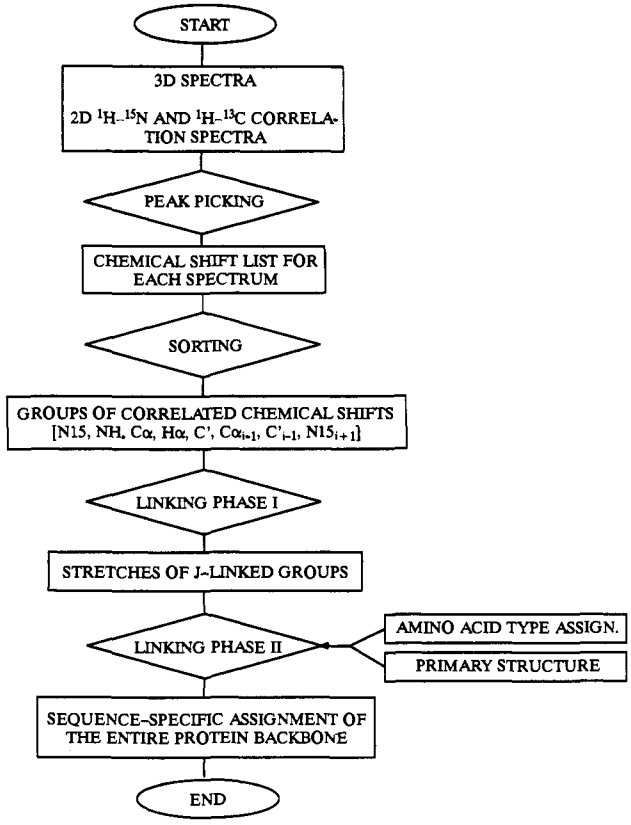

Figure 13. Flow diagram of the semiautomated assignment procedure, applied to calmodulin[12] (reprinted from ref 12).

C. Peak Analysis in *n*D

After a multidimensional spectrum has been detected and transformed, there is a very important question of peak assignment and quantification. Assignment has been mentioned already above. Quantification of peaks in a multidimensional spectrum, however, poses unusual problems in comparison with two-dimensional cases.

When dipolar magnetization transfer is connected with scalar transfer, as for example, in homonuclear 3D HOHAHA-NOESY[9] or TOCSY-NOESY[80] experiments, cross-peak volumes compress information from both steps. However, this increased complexity can provide extra information about the secondary structure of the molecule.[9,80] Such complications are even more likely if more dimensions are involved.

Accurate volumes of cross-peaks for as many distance constraints as possible are simultaneous tasks for peak analysis in multi-dimensional NMR. The resulting data then can be used for achieving better molecular structure through various computer programs (e.g. IRMA,[159,160] CORMA, and MARDIGRAS[161]). General problems of volume measurements[160,162] will not be addressed here in detail.

Volume measurement for multidimensional correlation peaks, however, is most straightforward using digital integration, i.e. summation of all intensity present in the volume around the cross-peak. Such quantification is the best way to get the most error-free volumes even with low digital resolution and the presence of residual zero-quantum effects.[160,163] Some difficulties may arise because of the large line widths of 3D peaks. However, it was shown theoretically[164] that if Gaussian filtering is used, the bias and variance of integrals are reduced in comparison to the case of Lorentzian line shapes. This finding was successfully used recently in integration of 3D TOCSY-NOESY spectra of proteins,[80] where the error of measured integrals was found to be within 5%. Recently a semiautomatic integration program was also developed for overlapping peaks[165] which is a simple 2D line fit, preferably also for Gaussian line shapes. A deconstruction method was also proposed to resolve overlapping NOE correlation peaks.[166]

Peak (curve) fitting was found preferable in analyzing 1D spectra, if the analytical form of the peaks is known. Numerical integration underestimates the real area due to the noise, digitization errors, and finite truncation of peak tails.[167] Unfortunately the success of peak-fitting procedures is very dependent on initial conditions. Recently the Metropolis or simulated annealing algorithm was shown to be advantageous for curve-fitting spectra with severe problems, such as badly defined base line (roll), diverse line width, and poor initial estimates of parameters.[168] This algorithm reliably finds the global minima of the spectral parameters. The only problem seems to be the huge computational requirement. For a relatively simple 1D spectrum the calculation can take a half hour on a minisupercomputer.[168] Furthermore it suffers from the same drawback as every line fitting procedure: the peak shapes should be analytically defined, which is not easily fulfilled for multidimensional data. Consequently, such volume determination still awaits more developed computer programs and computational power.

VII. Future and Present Time

Processing of multidimensional NMR data is a big challenge for the present time and for the very next future. Just five years ago[169] envisioning the future for the 1990s it was natural to foresee a typical working place for NMR spectroscopists to handle their data on hardware with high CPU performance, large data storage media, wide I/O bandwidth, on-line supercomputer support, and high performance graphics. Now here we are in those bright years and indeed the hardware has developed quite in the predicted manner. Nevertheless, some of the goals are only approached and not yet achieved. While this is true for well equipped facilities, the bitter reality is that the sophistication of hardware in many laboratories cannot keep pace with top-of-the-line computers simply because of financial problems. Even worse, the computational needs have been increasing in nonpredictable ways.

With 4D NMR measurements, and certainly with 5D and 6D under way, the data processing requirements pose serious tasks for all but high-end computers. As an example, one of the first high-resolution 3D data sets processed on an Aspect 1000 computer took 7 h[23] and four years ago that was the mainstream computer at many NMR laboratories. Processing the first, 4D $^{13}C/^{15}N$-edited NOESY experiment with an acquisition size of 16 (complex) × 64 (complex) × 16 (complex) × 512 (real) took 12 h for just the t_3 dimension with one zero fill.[16] The resultin 32 3D data sets needed an additional 1 to 2 h to process each, with equal amounts of double zero filling in t_1, t_2 and t_4, respectively. This

roughly 60-h session was accomplished on a Sun Sparcstation (in local mode),[16] which is a mainstream computer of today's laboratory. Just recently a 4D FFT combined with linear prediction extrapolation took 62 h on a "top-of-the-line" computer, a Silicon Graphics 4D/220.[17] Output size of such spectra reaches easily the gigabyte range. The software used for this enormous tasks are now totally in-house written,[17] or a result of mixing existing software with in-house routines.[16,18,61] The conclusions are clear: changes in the strategy, hardware, and software are required for multidimensional NMR processing to be accessible for many laboratories. These aspects are closely related with some of the possible solutions listed below.

If there is an existing network of computers in the vicinity of an NMR laboratory, then data processing software can distribute subtasks for processing among idle computers, speeding up the overall application. For this strategy there are many unsolved questions, and only the first results have appeared.[39] A widely appreciated and general solution is yet to come.

A second strategy is possible if there is a supercomputer accessible to the NMR laboratory. Although results of using minisupercomputers for NMR processing (e.g., for 1D,[170] for 2D,[171] and for 3D[150]) have been published this option is not generally available at this time. There are also problems due to hardware, operating system and word format incompatibilities. The use of a "departmental", minisupercomputer or even a large mainframe computer is also desirable. It will also be necessary to evaluate the relative effectiveness of a computer with a few scalar + vector processors[150,170,171] in contrast to a massively parallel computer.[37,39] Moreover, the existing commercial software has no capability to fully utilize these computers. The best solutions will evolve over time and are presently difficult to forecast because there are so few published results.

However, some preliminary results show the usage of a massively parallel digital computer in 3D processing to be very promising (e.g., 3D FFT for 256 × 256 × 256 × 2 points size test data in 10 s on 8192 processors on a Connection Machine[39]). There are several other promising possibilities including optical or optoelectric hybrid computers. By using these types of computers, after an appropriate translation of multidimensional data, Fourier transforms would take only nanoseconds (since the data processing speed is roughly governed by the speed of light passing through optical devices[172]). That is really a futuristic vision!

Array processors could be a relatively cheap alternative for parallel/supercomputers. Array processors have been in use for some time, and recent promising results were shown for processing 2D and 3D[103] spectra on inexpensive array processors attached to a personal computer. However, there is a barrier to usage, namely the existing software should be adapted to each available type of array processor (hardware and software), requiring considerable programming effort.

It is obvious that forecasting future hardware trends is a hazardous endeavor. Perhaps more hazardous is the plight of the laboratories faced with an expensive budget choice, who could purchase a machine that is next year's "orphan". Recent history demonstrates that even a conservative choice results in the obsolescence of a machine within five years of its purchase. At the present time, given the convergence of NMR data processing and molecular modeling, many laboratories are opting for computers with large data throughout capacity—for NMR processing and molecular mechanics—as well as the interactive graphics capability currently used to evaluate candidate structures. Other contributions to this issue of *Chemical Reviews* provide ample demonstration of this trend.

VIII. Acknowledgments

The authors are very indebted to Dr. Istvân T. Horváth (EXXON, Corporate Research) encouraging preparation of this work. Special thanks are due to Prof. P. N. Borer (Syracuse University and New Methods Research, Inc., Syracuse, NY) for critical reading of the manuscript and for many stimulating discussions. Kind help of Prof. James Swinehart (SUNY, Cortland) is greatly appreciated. The authors are very thankful to all who have sent preprints or reprints of their results: Prof. R. Freeman (Cambridge University, England), Dr. H. Oschkinat (Max-Planck-Institut für Biochemie, Germany), Dr. E. R. P. Zuiderweg (Abbott Laboratories), Prof. A. A. Bothner-By (Carnegie Mellon University), Prof. A. Pines (University of California, Berkeley), Dr. K. Nagayama (JEOL Ltd., Japan), and Prof. G. C. Levy (Syracuse University). Discussions with Prof. C. Griesinger (J. W. Goethe—Universität Frankfurt, Germany) were very helpful. Permissions from the authors and from the publishers for reproducing figures and original copies are greatly appreciated. This project was partly supported by the Biomedical Research Technology Program of the Division of Research Resources of NIH (Grant RR-1317 to G. C. Levy) and by the NIH (Grant GM-32691 to P. N. Borer). Support from Office of Sponsored Programs and Chemistry Department, Syracuse University, is appreciated.

IX. References

(1) Ernst, R. R. *Chimia* **1975**, *29*, 179.
(2) Fukushima, E.; Roeder, S. B. W. *Experimental Pulse NMR. A Nuts and Bolts Approach*; Addison-Wesley Publishing Company, Inc.: London, 1981.
(3) Bax, A. *Two-Dimensional Nuclear Magnetic Resonance in Liquids*; Reidel: Boston, 1982.
(4) Ernst, R. R.; Bodenhausen, G.; Wokaun, A. *Principles of Nuclear Magnetic Resonance in One and Two Dimensions*; Clarendon: Oxford, 1986.
(5) Levy, G. C. *J. Chem. Inf. Comp. Sci.* **1988**, *28*, 167.
(6) Craik, D. J.; Brownlee, R. T. C. Graphics-aided NMR. In *Annual Reports on NMR Spectroscopy*; Webb, G. A., Ed.; Academic Press: London, 1989, Vol. 21.
(7) Levy, G. C. Computer-Enhanced Nuclear Magnetic Resonance Spectroscopy. In *Computer-Enhanced Analytical Spectroscopy*; Meuzelaar, H. L. C., Ed.; Plenum Publishing Co.: Washington, 1990, Vol. 2.
(8) Griesinger, C.; Sørensen, O. W.; Ernst, R. R. *J. Magn. Reson.* **1989**, *84*, 14.
(9) Oschkinat, H.; Cieslar, C.; Holak, T. A.; Clore, G. M.; Gronenborn, A. M. *J. Magn. Reson.* **1989**, *83*, 450.
(10) Fesik, S. W.; Zuiderweg, E. R. P. *Quart. Rev. Biophys.* **1990**, *23*, 97.
(11) Wagner, G. *Prog. Nucl. Magn. Reson. Spectrosc.* **1990**, *22*, 101.
(12) Ikura, M.; Kay, L. E.; Bax, A. *Biochemistry* **1990**, *29*, 4659.
(13) Wagner, G.; Schmieder, P.; Thanabal, V. *J. Magn. Reson.* **1991**, *93*, 436.
(14) Bax, A.; Ikura, M. *J. Biomol. NMR* **1991**, *1*, 99.
(15) Fesik, S. W.; Eaton, H. L.; Olejniczak, E. T.; Gampe, R. T., Jr. *J. Am. Chem. Soc.* **1990**, *112*, 5370.
(16) Kay, L. E.; Clore, G. M.; Bax, A.; Gronenborn, A. M. *Science* **1990**, *249*, 411.

(17) Zuiderweg, E. R. P.; Petros, A. M.; Fesik, S. W.; Olejniczak, E. T. *J. Am. Chem. Soc.* **1991**, *113*, 370.
(18) Clore, G. M.; Kay, L. E.; Bax, A.; Gronenborn, A. M. *Biochemistry* **1991**, *30*, 12.
(19) Kay, L. E.; Ikura, M.; Zhu, G.; Bax, A. *J. Magn. Reson.* **1991**, *91*, 422.
(20) Sørensen, O. W. *J. Magn. Reson.* **1990**, *89*, 210.
(21) Sørensen, O. W. *J. Magn. Reson.* **1990**, *90*, 433.
(22) Blümich, B. *Prog. Nucl. Magn. Reson. Spectrosc.* **1987**, *19*, 331.
(23) Griesinger, C.; Sørensen, O. W.; Ernst, R. R. *J. Am. Chem. Soc.* **1987**, *109*, 7227.
(24) Davies, S.; Friedrich, J.; Freeman, R. *J. Magn. Reson.* **1988**, *76*, 555.
(25) Freeman, R. *Chem. Rev.* **1991**, *91*, (this issue).
(26) Wijmenga, S. S.; Hilbers, C. W. *J. Magn. Reson.* **1990**, *88*, 627.
(27) Majumdar, A.; Hosur, R. V. *J. Magn. Reson.* **1990**, *90*, 597.
(28) Clore, G. M.; Grorenborn, A. *Science* **1991**, *252*, 1390.
(29) Wider, G.; Neri, D.; Otting, G.; Wüthrich, K. *J. Magn. Reson.* **1989**, *85*, 426.
(30) Wider, G.; Weber, C.; Traber, R.; Widmer, H.; Wüthrich, K. *J. Am. Chem. Soc.* **1990**, *112*, 9015.
(31) Cavanagh, J.; Rance, M. *J. Magn. Reson.* **1990**, *88*, 72.
(32) Cavanagh, J.; Palmer, A. G., III; Wright, P.; Rance, M. *J. Magn. Reson.* **1991**, *91*, 429.
(33) Delsuc, M. A.; Lallemand, J. Y. *J. Magn. Reson.* **1986**, *69*, 504.
(34) Bax, A.; Clore, G. M.; Driscoll, P. A.; Gronenborn, A. M.; Ikura, M.; Kay, L. E. *J. Magn. Reson.* **1990**, *87*, 620.
(35) Bax, A.; Clore, G. M.; Gronenborn, A. *J. Magn. Reson.* **1990**, *88*, 425.
(36) Zhu, G.; Bax, A. *J. Magn. Reson.* **1990**, *90*, 405.
(37) Denning, P. J.; Tichy, W. F. *Science* **1990**, *250*, 1217.
(38) Hoffman, R. E.; Levy, G. C. *Comput. Chem.* **1989**, *13*, 179.
(39) Levy, G. C.; Wang, S.; Kumar, P.; Borer, P. N. *Spectroscopy* **1991**, *6*, 22.
(40) For a recent listing of available NMR software see: *Methods of Enzymology*; Oppenheimer, N. J., James, T. L., Eds.; Academic Press: San Diego, CA, 1989; Vols. 176 and 177.
(41) Braunschweiler, L.; Ernst, R. R. *J. Magn. Reson.* **1983**, *53*, 521.
(42) Bax, A.; Davis, D. G. *J. Magn. Reson.* **1985**, *65*, 355.
(43) Kay, L. E.; Ikura, M.; Tschudin, R.; Bax, A. *J. Magn. Reson.* **1990**, *89*, 496.
(44) Kay, L. E.; Ikura, M.; Bax, A. *J. Magn. Reson.* **1991**, *91*, 84.
(45) Kay, L. E.; Ikura, M.; Bax, A. *J. Am. Chem. Soc.* **1990**, *112*, 888.
(46) Marion, D.; Ikura, M.; Tschudin, R.; Bax, A. *J. Magn. Reson.* **1989**, *85*, 393.
(47) (a) Pelczer, I. *J. Am. Chem. Soc.* **1991**, *113*, 3211. (b) Friedrichs, M. S.; Metzler, W. J.; Mueller, L. *J. Magn. Reson.*, in press.
(48) Kurihara, N.; Kamo, O.; Umeda, M.; Sato, K.; Hyakuna, K.; Nagayama, K. *J. Magn. Reson.* **1985**, *65*, 405.
(49) Fesik, S. W.; Eaton, H. L.; Olejniczak, E. T.; Zuiderweg, E. R. P. *J. Am. Chem. Soc.* **1990**, *112*, 886.
(50) Barna, J. C. J.; Laue, E. D.; Mayger, M. R.; Skilling, J.; Worrall, S. J. P. *Biochem. Soc. Trans.* **1986**, *14*, 1262.
(51) Barna, J. C. J.; Laue, E. D.; Mayger, M. R.; Skilling, J.; Worrall, S. J. P. *J. Magn. Reson.* **1987**, *73*, 69.
(52) Keeler, J.; Neuhaus, D. *J. Magn. Reson.* **1985**, *63*, 454.
(53) Bax, A.; Marion, D. *J. Magn. Reson.* **1988**, *78*, 186.
(54) Nagayama, K. *J. Magn. Reson.* **1986**, *69*, 508.
(55) Redfield, A. G.; Kunz, S. D. *J. Magn. Reson.* **1975**, *19*, 250.
(56) Drobny, G.; Pines, A.; Sinton, S.; Weitekamp, D.; Wemmer, D. *Faraday Discuss. Chem. Soc. Symp.* **1979**, *13*, 49.
(57) Bodenhausen, G.; Vold, R. L.; Vold, R. R. *J. Magn. Reson.* **1980**, *37*, 93.
(58) Marion, D.; Wüthrich, K. *Biochem. Biophys. Res. Commun.* **1983**, *113*, 967.
(59) (a) Müller, L.; Ernst, R. R. *Mol. Phys.* **1979**, *38*, 963. (b) States, D. J.; Haberkorn, R. A.; Ruben, D. J. *J. Magn. Reson.* **1982**, *48*, 286.
(60) Bax, A. *Bull. Magn. Reson.* **1985**, *7*, 167.
(61) Kay, L. E.; Marion, D.; Bax, A. *J. Magn. Reson.* **1989**, *84*, 72.
(62) Simorre, J.-P.; Marion, D. *J. Magn. Reson.* **1990**, *89*, 191.
(63) Freeman, R. *A Handbook of Nuclear Magnetic Resonance*; Longman: Harlow, 1988.
(64) Marion, D.; Bax, A. *J. Magn. Reson.* **1988**, *79*, 352.
(65) Marion, D.; Kay, L. E.; Sparks, S. W.; Torchia, D. A.; Bax, A. *J. Am. Chem. Soc.* **1989**, *111*, 1515.
(66) Ikura, M.; Kay, L. E.; Tschudin, R.; Bax, A. *J. Magn. Reson.* **1990**, *86*, 204.
(67) Clore, G. M.; Bax, A.; Driscoll, P.; Wingfield, P. T.; Gronenborn, A. *Biochemistry* **1990**, *29*, 8172.
(68) Vuister, G. W.; de Waard, P.; Boelens, R.; Vliegenthart, J. F. G.; Kaptein, R. *J. Am. Chem. Soc.* **1989**, *111*, 772.
(69) Wijmenga, S. S.; Hallenga, K.; Hilbers, C. W. *J. Magn. Reson.* **1989**, *84*, 634.
(70) Davis, D. G. *J. Magn. Reson.* **1989**, *81*, 603.
(71) Frenkiel, T.; Bauer, C.; Carr, M. D.; Birdsall, B.; Feeney, J. *J. Magn. Reson.* **1990**, *90*, 420.
(72) Otting, G.; Wider, H.; Wagner, G.; Wüthrich, K. *J. Magn. Reson.* **1986**, *66*, 187.
(73) Marion, D.; Bax, A. *J. Magn. Reson.* **1989**, *83*, 205.
(74) Bax, A.; Ikura, M.; Kay, L. E.; Zhu, G. *J. Magn. Reson.* **1991**, *91*, 174.
(75) Zuiderweg, E. R. P.; McIntosh, L. P.; Dahlquist, F. W.; Fesik, S. W. *J. Magn. Reson.* **1990**, *86*, 210.
(76) Zuiderweg, E. R. P.; Fesik, S. W. *Biochemistry* **1989**, *28*, 2387.
(77) Padilla, A.; Vuister, G. W.; Boelens, R.; Kleywegt, G. J.; Cavé, A.; Parello, J.; Kaptein, R. *J. Am. Chem. Soc.* **1990**, *112*, 5024.
(78) Driscoll, P. C.; Gronenborn, A. M.; Wingfield, P. T.; Clore, G. M. *Biochemistry* **1990**, *29*, 4668.
(79) Rinaldi, P. L.; Tokles, M.; Coker, D. 31st ENC, Asilomar, Pacific Grove, CA, April 1–5, 1990; Poster MP45.
(80) Oschkinat, H.; Cieslar, C.; Griesinger, C. *J. Magn. Reson.* **1990**, *86*, 453.
(81) Kessler, H.; Schmieder, P.; Oschkinat, H. *J. Am. Chem. Soc.* **1990**, *112*, 8599.
(82) Schneider, P.; Kessler, H.; Oschkinat, H. *Angew. Chem., Int. Ed. Engl.* **1990**, *29*, 546.
(83) Boelens, R.; Vuister, G. W.; Koning, T. M. G.; Kaptein, R. *J. Am. Chem. Soc.* **1989**, *111*, 8525.
(84) Vuister, G. W.; Boelens, R.; Kaptein, R. *J. Magn. Reson.* **1988**, *80*, 176.
(85) Fesik, S. W.; Zuiderweg, E. R. P. *J. Magn. Reson.* **1988**, *78*, 588.
(86) Nagayama, K.; Yamazaki, T.; Yoshida, M.; Kanaya, S.; Nakamura, H. *J. Biochem.* **1990**, *108*, 149.
(87) Marion, D.; Driscoll, P. C.; Kay, L. E.; Wingfield, P. T.; Bax, A.; Gronenborn, A. M.; Clore, G. M. *Biochemistry* **1989**, *28*, 6150.
(88) Driscoll, P. C.; Clore, G. M.; Marion, D.; Wingfield, P. T.; Gronenborn, A. M. *Biochemistry* **1990**, *29*, 3542.
(89) Clore, G. M.; Bax, A.; Wingfield, P. T.; Gronenborn, A. M. *Biochemistry* **1990**, *29*, 5671.
(90) Breg, J. N.; Boelens, R.; Vuister, G. W.; Kaptein, R. *J. Magn. Reson.* **1990**, *87*, 646.
(91) Szalma, S.; Pelczer, I.; Borer, P. N.; Levy, G. C. *J. Magn. Reson.* **1991**, *91*, 194.
(92) Lindon, J. C.; Ferrige, A. G. *Prog. Nucl. Magn. Reson. Spectrosc.* **1980**, *14*, 27.
(93) Led, J. J.; Gesmar, H. *Chem. Rev.* **1991**, *91*, 1413 (this issue).
(94) Olejniczak, E. T.; Eaton, H. L. *J. Magn. Reson.* **1990**, *87*, 628.
(95) Cieslar, C.; Holak, T. A.; Oschkinat, H. *J. Magn. Reson.* **1990**, *89*, 184.
(96) Ikura, M.; Bax, A.; Clore, G. M.; Gronenborn, A. M. *J. Am. Chem. Soc.* **1990**, *112*, 9020.
(97) Cieslar, C.; Clore, G. M.; Gronenborn, A. M. *J. Magn. Reson.* **1988**, *80*, 119.
(98) Marshall, A. G.; Roe, D. C. *Anal. Chem.* **1978**, *50*, 756.
(99) Roe, D. C.; Marshall, A. G.; Smallcombe, S. H. *Anal. Chem.* **1978**, *50*, 764.
(100) Craig, E. C.; Marshall, A. G. *J. Magn. Reson.* **1988**, *76*, 458.
(101) Hoffman, R. E.; Delaglio, F.; Levy, G. C. Unpublished work.
(102) Levitt, M. H.; Freeman, R. *J. Magn. Reson.* **1979**, *34*, 675.
(103) Zolnai, Zs.; Macura, S.; Markley, J. L. *J. Magn. Reson.* **1990**, *89*, 94.
(104) Ernst, R. R. *J. Magn. Reson.* **1969**, *1*, 7.
(105) Pelczer, I.; Bishop, K. D.; Levy, G. C.; Borer, P. N. *J. Magn. Reson.* **1991**, *91*, 604.
(106) Edwards, M. W.; Bax, A. *J. Am. Chem. Soc.* **1986**, *108*, 918.
(107) Bartholdi, E.; Ernst, R. R. *J. Magn. Reson.* **1973**, *11*, 9.
(108) Bax, A.; Byrd, R. A.; Aszalos, A. *J. Am. Chem. Soc.* **1984**, *106*, 7632.
(109) McLeod, K.; Comisarow, M. B. *J. Magn. Reson.* **1989**, *84*, 490.
(110) Ni, F.; Levy, G. C.; Scheraga, H. A. *J. Magn. Reson.* **1986**, *66*, 385.
(111) Ni, F.; Scheraga, H. A. *J. Magn. Reson.* **1989**, *82*, 413.
(112) Jeong, G.-w.; Borer, P. N. Private communication.
(113) Stephenson, D. S. *Prog. Nucl. Magn. Reson. Spectrosc.* **1988**, *20*, 515.
(114) Hoult, D. I.; Chen, C.-N.; Eden, H.; Eden, M. *J. Magn. Reson.* **1983**, *51*, 110.
(115) Sklenár, W.; Bax, A. *J. Magn. Reson.* **1987**, *74*, 469.
(116) Lippens, G.; Hallenga, K. *J. Magn. Reson.* **1990**, *88*, 619.
(117) Burg, J. P. In Proceedings of the 37th Meeting of Society of Exploration Geophysicists, Oklahoma City, OK, Oct 31, 1967.
(118) Press, W. H.; Flannery, B. P.; Teukolsky, S. A.; Vetterling, W. T. *Numerical Recipes: The Art of Scientific Computing*; Cambridge Univ. Press: Cambridge, 1986; Chapter 12.
(119) Kumaresan, R.; Tufts, D. W. *IEEE Trans. Acoust. Speech Signal Process.* **1982**, *30*, 833.
(120) (a) Henrichs, P. M.; Hewitt, J. M.; Young, R. H. *J. Magn. Reson.* **1986**, *69*, 460. (b) Heuer, A.; Haeberlen, U. *J. Magn. Reson.* **1989**, *85*, 79.
(121) Dietrich, W.; Rüdel, C. H.; Neumann, M. *J. Magn. Reson.* **1991**, *91*, 1.

(122) Zolnai, Zs.; Macura, S.; Marlkey, J. L. *J. Magn. Reson.* **1989**, *82*, 496.
(123) (a) Redfield, A. G.; Gupta, R. K. *J. Chem. Phys.* **1971**, *54*, 1418. (b) Adler, M.; Wagner, G. *J. Magn. Reson.* **1991**, *91*, 450.
(124) Tsang, P.; Wright, P. E.; Rance, M. *J. Magn. Reson.* **1990**, *88*, 210.
(125) Bielecki, A.; Levitt, M. H. *J. Magn. Reson.* **1989**, *82*, 562.
(126) Kuroda, Y.; Wada, A.; Yamazaki, T.; Nagayama, K. *J. Magn. Reson.* **1989**, *84*, 604.
(127) Kuroda, Y.; Wada, A.; Yamazaki, T.; Nagayama, K. *J. Magn. Reson.* **1990**, *88*, 141.
(128) Marion, D.; Ikura, M.; Bax, A. *J. Magn. Reson.* **1989**, *84*, 425.
(129) Mitschang, L.; Cieslar, C.; Holak, T. A.; Oschkinat, H. *J. Magn. Reson.* **1991**, *92*, 208.
(130) Ahmed, N.; Rao, K. R. *Orthogonal Transforms for Digital Signal Processing*; Springer: Berlin, 1975.
(131) Oschkinat, H.; Cieslar, C.; Mitschang, L.; Ross, A.; Holak, T. A.; Auerswald, E. *Bruker Report* **1990**, *2*, 2.
(132) Szalma, S.; Borer, P. N.; Levy, G. C.; Pelczer, I. Submitted for publication.
(133) Pelczer, I.; Borer, P. N.; Levy, G. C.; Szalma, S. Frontiers of NMR in Molecular Biology-II, Keystone, CO, April 8–14, 1991; Poster CG131.
(134) Hoch, J. C. In *Methods of Enzymology*; Oppenheimer, N. J., James, T. L., Eds.; Academic Press: San Diego, CA, 1989; Vol. 176.
(135) Jones, J. A.; Hore, P. J. *J. Magn. Reson.* **1991**, *92*, 276.
(136) Jones, J. A.; Hoare, P. J. *J. Magn. Reson.* **1991**, *92*, 363.
(137) Gesmar, H.; Led, J. J. *J. Magn. Reson.* **1988**, *76*, 575.
(138) Gesmar, H.; Led, J. J.; Abildgaard, F. *Prog. Nucl. Magn. Reson. Spectrosc.* **1990**, *22*, 255.
(139) (a) Grahn, H.; Edlund, U.; van den Hoogen, Y. Th.; Altona, C.; Delaglio, F.; Rogenbuck, M.; Borer, P. N. *J. Biomol. Struct. Dyn.* **1989**, *6*, 1135. (b) Hardy, J. K.; Rinaldi, P. L. *Magn. Reson.* **1990**, *88*, 320.
(140) Mitschang, L.; Neidig, K.-P.; Kalbitzer, H. R. *J. Magn. Reson.* **1990**, *90*, 359.
(141) Kumar, A. Private communication (software developed at Syracuse University).
(142) Tang, J.; Norris, J. R. *J. Magn. Reson.* **1988**, *79*, 190.
(143) Yan, H.; Gore, J. C. *J. Magn. Reson.* **1990**, *88*, 354.
(144) Boentges, S.; Meier, B. U.; Griesinger, C.; Ernst, R. R. *J. Magn. Reson.* **1989**, *85*, 337.
(145) Szalma, S. *J. Magn. Reson.* **1989**, *83*, 400.
(146) Neidig, K.-P.; Kalbitzer, H. R. *J. Magn. Reson.* **1990**, *88*, 155.
(147) Zolnai, Zs.; Macura, S.; Markley, J. L. *J. Magn. Reson.* **1988**, *80*, 60.
(148) Zolnai, Zs.; Westler, W. M.; Ulrich, E. L.; Medley, J. L. *J. Magn. Reson.* **1990**, *88*, 511.
(149) Delaglio, F. Private communication.
(150) Oschkinat, H.; Cieslar, C.; Gronenborn, A. M.; Clore, G. M. *J. Magn. Reson.* **1989**, *81*, 212.
(151) Pelczer, I.; Hoffman, R. E.; Levy, G. C. 31st ENC, Asillomar, Pacific Grove, California, April 1–5, 1990; Poster MP46.
(152) Fesik, S. W.; Gampe, Jr., R. T.; Zuiderweg, E. R. P. *J. Am. Chem. Soc.* **1989**, *111*, 770.
(153) Szalma, S.; Pelczer, I. *J. Magn. Reson.* **1988**, *76*, 416.
(154) Weber, P. L.; Mueller, L. *J. Magn. Reson.* **1989**, *81*, 430.
(155) Bock-Möbius, I. *J. Magn. Reson.* **1989**, *84*, 591.
(156) Roggenbuck, M. W.; Hyman, T. J.; Borer, P. N. In *Structure & Methods. Vol. 3*: Sarma, R. H., Sarma, M. H., Eds.; Adenine Press: Albany, 1990; Vol. 3 (*DNA & RNA*), p 309.
(157) Kleywegt, G. J.; Boelens, R.; Kaptein, R. *J. Magn. Reson.* **1990**, *88*, 601.
(158) Cieslar, C.; Holak, T. A.; Oschkinat, H. *J. Magn. Reson.* **1990**, *87*, 400.
(159) Boelens, R.; Koning, T. M. G.; Kaptein, R. *J. Mol. Struct.* **1988**, *173*, 299.
(160) Boelens, R.; Koning, T. M. G.; van der Marel, G. A.; van Boom, J. H.; Kaptein, R. *J. Magn. Reson.* **1989**, *82*, 290.
(161) Borgias, B. A.; Gochin, M.; Kerwood, D. J.; James, T. L. *Prog. Nucl. Magn. Reson. Spectrosc.* **1990**, *22*, 83.
(162) Zhou, N.; Bianucci, A. M.; Pattabiraman, N.; James, T. L. *Biochemistry* **1987**, *26*, 7905.
(163) Wang, K.-Y.; Borer, P. N.; Levy, G. C.; Pelczer, I. *J. Magn. Reson.*, in press.
(164) Weiss, G. H.; Ferretti, J. A.; Byrd, R. A. *J. Magn. Reson.* **1987**, *71*, 97.
(165) Gochin, M.; Zon, G.; James, T. L. *Biochemistry* **1990**, *29*, 11161.
(166) McIntyre, L.; Freeman, R. *J. Magn. Reson.* **1990**, *89*, 639.
(167) Weiss, G. H.; Ferretti, J. A. *J. Magn. Reson.* **1983**, *55*, 397.
(168) Hoffman, R. E.; Levy, G. C. *J. Magn. Reson.* **1989**, *83*, 411.
(169) Levy, G. C.; Delaglio, F.; Macur, A.; Begemann, J. *Comp. Enh. Spectrosc.* **1986**, *3*, 1.
(170) Hoffman, R. E.; Levy, G. L. *J. Magn. Reson.* **1989**, *83*, 411.
(171) Hoffman, R. E.; Kumar, A.; Bishop, K. D.; Borer, P. N.; Levy, G. C. *J. Magn. reson.* **1989**, *83*, 586.
(172) For a recent survey on optical computing see for example: Feitelson, D. G. *Optical Computing, A Survey for Computer Scientists*; MIT Press: Cambridge, 1988.
(173) Borer, P. N.; Pelczer, I.; Roggenbuck, M. W.; Wang, K.-Y.; Jeong, G.-w.; Bishop, K. D.; Gott, J.; Uhlenbeck, O. C. Frontiers of NMR in Molecular Biology-II, Keystone, CO, April 8–14, 1991; Poster CG202.
(174) Vuister, G. W. *Homonuclear Three-Dimensional NMR Spectroscopy of Biomolecules*. Ph.D. Thesis, Uthrecht, The Netherlands, 1991.